Politecnico di Torino

Master of Science in Aerospace Engineering

Structural and Thermal Prognostics and Diagnostics with Fiber Bragg Gratings

Main Supervisor: Prof. Ing. Paolo Maggiore
Co-Supervisors:

- Ing. Matteo Davide Lorenzo Dalla Vedova
- Ing. Daniel Milanese
- Ing. Davide Luca Janner

<div align="right">

Candidate: Scolpito Teo
S221955

</div>

A.A 2018/2019

"Non bisogna limitarsi ai risultati per valutare cosa viene fatto,

il successo non sono solo i risultati.

Sono le Difficoltà che vengono affrontate per ottenerli,

la Lotta Permanente e

lo Spirito per porsi ogni giorno nuove sfide e anche il Coraggio di Superarli.

El Camino es la Recompensa."

Óscar Washington Tabárez Silva

Index

List of Figures

List of Tables

Sommario

L'esigenza dell'industria aeronautica di disporre di strutture leggere e ad alte prestazioni ha fornito un forte impulso allo sviluppo di tecnologie in grado di ridurre il peso globale della macchina al fine di aumentarne l'efficienza e di ridurne i costi.

L'attività di ricerca condotta in questa tesi è volta allo studio e all'ottimizzazione di alcuni sistemi di bloccaggio per l'utilizzo di fibre ottiche come sensori e alla validazione dei sensori stessi.

Essi presentano molteplici peculiarità che li rendono candidati ideali per le applicazioni aeronautiche, fra cui in primis il peso e le dimensioni ridotte che permettono una comoda installazione senza invasività. A queste doti si aggiungono la capacità di multiplexing di più sensori sulla stessa fibra, di poter utilizzare la stessa fibra per la trasmissione dati e l'immunità alle interferenze elettromagnetiche.

Esistono diversi tipi di sensori che utilizzano le fibre ottiche. Nel nostro caso si sono utilizzati sensori di deformazione basati sui reticoli di Bragg.

Questi sensori sono costituiti da un reticolo fotoinciso all'interno della fibra che ha la capacità di riflettere solo alcune lunghezze d'onda della luce incidente. Se le proprietà geometriche del reticolo cambiano sotto l'effetto di un fattore esterno, cambia anche la forma dello spettro riflesso.

Nella prima parte del lavoro si è descritta la base teorica necessaria a raggiungere gli obbiettivi inizialmente fissati. In particolare si sono analizzate:

- Le caratteristiche principali delle fibre ottiche e le relative leggi fisiche che le governano;
- Le caratteristiche principali dei sensori, la loro tecnologia di realizzazione e le leggi che legano la variazione di lunghezza con le varie grandezze che essi possono analizzare;
- La teoria sulle misurazioni meccaniche che permette l'identificazione dei vari tipi errori commessi in fase di misurazione;
- La teoria statistica da utilizzare per la valutazione dell'errore.

Nella seconda parte sono esposte le scelte progettuali e costruttive prese durante la realizzazione del banco prova. La natura "propedeutica" della nostra ricerca ci ha imposto di scegliere un equipaggiamento adattabile alle diverse situazioni che si possono presentare in futuro. In particolar modo sono stati sviluppati sistemi di bloccaggio intercambiabili che permetto la sostituzione dell'elemento bloccante e degli elementi termici ad altezza variabile. Tutti gli elementi inoltre devono essere in grado di funzionare in maniera combinata tra di loro.

Viene inoltre brevemente descritto il codice di calcolo sviluppato per l'elaborazione dei

dati ottenuti dal sistema di interrogazione collegato al banco prova.

Nella terza ed ultima parte vengono descritte le prove eseguite con i mezzi di bloccaggio scelti ed i risultati ottenuti.

Essendo il nostro compito quello di creare la struttura base per l'attività di ricerca seguente, nel corso della trattazione sono esposti alcuni suggerimenti per i prossimi candidati che proseguiranno il nostro lavoro.

Summary

Aeronautical industry's needs to have light and high performance structures has given a strong impetus to the development of technologies able to reduce the overall weight of the machine in order to increase its efficiency and to reduce cost.

The research activity carried out in this thesis is aimed at the study and optimization of some locking systems for the use of optical fibers as sensors and for the validation of the sensors themselves.

They have many distinctiveness that make them ideal candidates for aeronautical applications, among which first the weight and the reduced dimensions that allow a comfortable installation without invasiveness. Added to these qualities is the ability to multiplexing multiple sensors on the same fiber, to use the same fiber for data transmission and immunity to electromagnetic interference.

There are several types of sensors that use optical fibers. In our case we used strain sensors based on Bragg gratings.

These sensors consist of a photoengraved grid within the fiber that can reflect only a few wavelengths of the incident light. If the geometric properties change under the influence of an external factor, the shape of the reflected spectrum also changes.

In the first part of the work we have described the theoretical basis necessary to achieve the objectives initially set. In particular, we analyzed:

- The main characteristics of optical fibers and the related physical laws that govern them;
- The main characteristics of the sensors, their realization technology and the laws that link the variation in length with the various quantities that they can analyze;
- The theory of mechanical measurements that allows the identification of the various types of errors committed during measurement;
- The statistical theory to be used for the evaluation of the error.

In the second part the design and construction choices taken during the test bench are exposed. The "propaedeutic" nature of our research has forced us to choose an equipment that can be adapted to the different situations that may arise in the future. Interchangeable locking systems have been developed that allow the replacement of the blocking element and of the variable height thermal elements. All elements must also be able to function in combination with each other.

It is also briefly described the calculation code developed for processing the data obtained from the interrogation system connected to the test bench.

In the third and last part, the tests performed with the selected locking means and the

results obtained are described.

Since it is our task to create the basic structure for the following research activity, during the discussion some suggestions are made for the next candidates who will continue our work.

1. Introduction

Usage of fiber optics is common in several applications today, mainly in telecommunication and sensors.

In the telecommunications field, they permit to have many advantages such as the possibility to transmit big data with high bit rate for long distance.

Therefore, data transmission is with low losses and there is no need to external power supply.

In addition, the fiber optics are immune to electromagnetic interference and characterized by high temperature and corrosive environment resistance: so, can be used in harsh environments like oceans floor.

Fiber optics used in sensors application are called Optical Fiber Sensors (OFS) and have the same properties, characteristics and advantages of the telecommunication ones.

In particular the subject of this work is a type of OFS: the Fiber Bragg Grating (FBG) sensors.

This kind of sensor has been used in some engineering applications, from Civil to Aerospace, and allows to measure strain, temperature, pressure and vibration.

These physical quantities are computed by using appropriate equations relating these quantities and wavelength variations detected by FBG.

1.1 Objectives

The main aim is to test FBG sensors and to design different types of locking systems.
Four main Steps can be identified:

1. Design and Manufacture Locking System
2. Assembly a Test Bench
3. Perform measuring campaign to evaluate the performance of the FBG sensors and of the locking system
4. Compare the obtained Result and choose the optimum system.

2. Optical Fibers

In addition to the well-known application in the field of telecommunication, it is possible to use optical fiber as sensors. Aeronautical and Space engineering can optimally exploit the advanteges that fibers give (low weight and high precision).

The main feature of the fiber is the ability to carry the light inside the core with a minimum signal attenuation: the value of the lowest loss is only 0.2 $dBkm^{-1}$ [1].

2.1 Materials

The most of common fiber optics are made of glass or plastic material. The choice of the material is given by the purpose of the application. In fact, the plastic optical fibers (POF), by having high attenuation, are used for short-distance applications and with low-bit-rate transmission systems [2] and are cheaper and more flexible than glass fibers [2].

Glass fibers have a low transmission optical loss, so they are used for long distance applications and when it has a high bit rate of transmission. Glass can be doped to increase or reduce the refractive index. Usually, to increase refractive index are used something like Germanium dioxide GeO_2, Phosphorus pentoxide P_2O_5, Titanium dioxide TiO_2 and Aluminium oxide Al_2O_3, on the other hand to reduce refractive index Boron trioxide B_2O_3 and Fluorine F can be used [3]. For example, GeO_2 and P_2O_5 have the peculiarity to increase the refractive index so they are suitable for fiber core [4], on the other hand dopants such as F and B_2O_3 are suitable for cladding because they decrease the refractive index [4].

2.2 Geometry and Basic Classification

The fiber optic has a cylindrical geometry and it is constituted by a core, a cladding and an external coating, see figure 1.
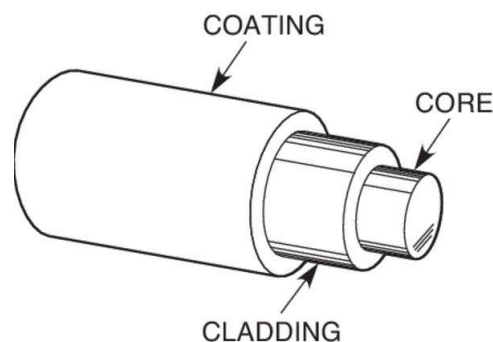
Figure 1: Optical Fiber Structure [2018 - Newport Corporation. All right reserved]

An initial classification of the fiber optics can be made based on modes of light propagation. So, it is possible to distinguish:

- Single-Mode (SI) fiber optic
- Multi-Mode (MM) fiber optic

The Single-mode fiber optic supports only one propagation mode and has a core thiner than the Multi-mode fibers (MM) core, as shown in figure 2[5]. In fact, the second one has a core diameter of about 50 μm (or more), instead the SI fibers have a core diameter of about 10 μm.

The dimension of the cladding is 125 μm and this value is standardised for all type of fiber optics.

Thanks to the large Numerical Aperture[1] [6] of a MM fiber, more light can be sent inside the fiber by using an inexpensive optical source such as a LED [2]. Therefore, by having a large core, this fiber class is easier to splice than SI fibers.

On the other hand, MM fiber optics have some disadvantages. Due to intermodal dispersion[2] [7], they are not suitable for long-haul and/or in applications with a high bit-rate where SI fibers are preferable because they permits haul from 1000 km to 30000 km and a high-bit-rate from 10 Gb/s to 100 Gb/s [3].

Another classification of the fiber optics is based on the refractive index of core:

- *Step index fiber*
- *Graded index fiber*

Different type of fiber are shown in figure 2 below [5].

In the first type of fiber class, by calling r_1 radius core and r_2 radius cladding, there are various diameter ratios: 8/125, 50/125, 62.5/125, 85/125 and 100/140 [$\mu m/\mu m$] [8]. In this class of fiber, the refractive index of core and cladding are costant and uniform. The refractive index drastically changes to core-cladding interface but n_1 and $n2$ are slight different. This slight difference between the value of those index, is obtained by adding a low concentration of dopant [8].

In the graded index fibers the refrective index of the cladding is constant and uniform but the refractive index of the core changes gradually, nearly parabolic, with a maximum value along the axis of fiber until the minimum value along the core-cladding interface.

---

[1] The **numerical aperture** (NA) of an optical system is a dimensionless number that characterizes the range of angles over which the system can accept or emit light. By incorporating index of refraction in its definition, NA has the property that it is constant for a beam as it goes from one material to another, provided there is no refractive power at the interface.

[2] **Modal dispersion** is a distortion mechanism occurring in multimode fibers and other waveguides, in which the signal is spread in time because the propagation velocity of the optical signal is not the same for all modes.
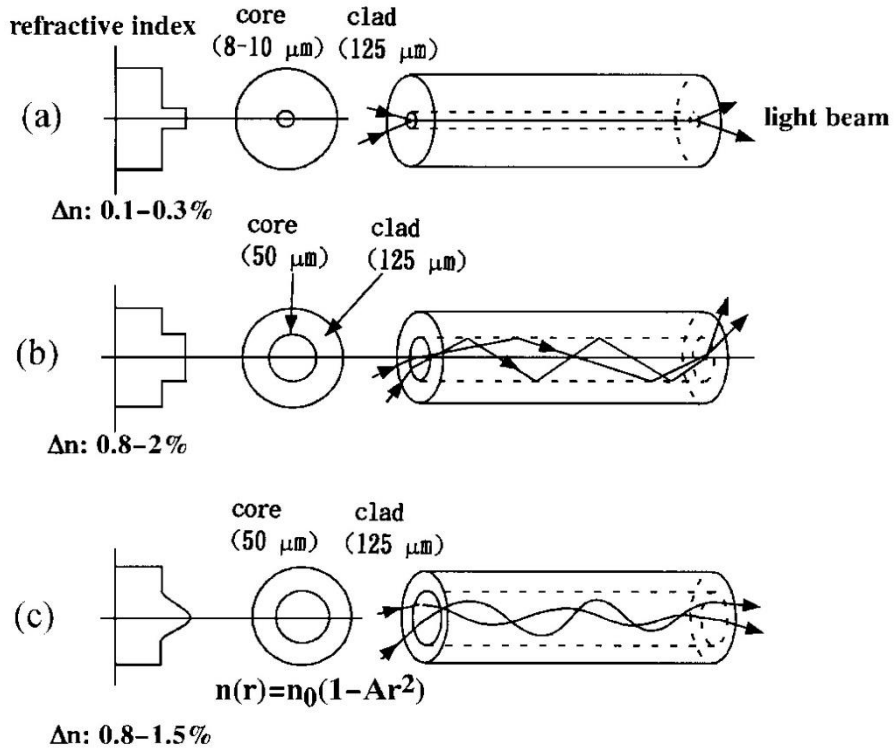
Figure 2: Different Type of Fibers. (a) SI , (b) MM Step Index, (c) MM Graded Index

Consequently, the refractive index of the core is a function of *r*, where *r* is the radial position.

Materials for Graded index fibers, are obtained by adding dopants in a correct concentrations [8], and because of this particular variation of refractive index the optical ray does not follow a straight line along the fiber but a curved line. The general function that describes the refractive index variation of graded index fibers, it is the following relation [8]:

$$n^2(r) = n_1^2 \left[1 - 2 \left(\frac{r}{a}\right)^p \Delta\right.$$

Where *p* is called *grade profile parameter* and by varying his value from 1 to infinite it is possible to obtain different refractive profile, and *Δ* is the *normalized refractive index*.

2.3 Physical Principles behind Fiber Optics

The propagation of light into the fiber core is based on the *Total Internal Reflection* (TIR). This phenomenon takes place when the light strikes a medium with an angle larger than the Critical Angle[3] and the refractive index of the core is higher than refractive index of the cladding. In this way, light cannot pass through and is totally reflected.

Refractive index is computed with the following equation:

$$n = \frac{c}{v}$$

- *n*=refractive index of medium;
- v=speed of light (in medium);
- *c*=speed of light (in vacuum).

In accordance with the optical phenomenon above descripted, it is necessary to introduce the fundamental Snell's Law:

$$n_1 \cdot sin(\alpha_i) = n_2 \cdot sin(\alpha_r)$$

Where:

- n_1= refractive index of the first medium;
- n_2=refractive index of second medium;
- α_i=incidence angle;
- α_r=refractive angle.

The Critical (or Limit) angle is defined by:

$$\theta_c = \arcsin\frac{n_2}{n_1}$$

This angle is obtained when the refractive angle α_r is 90°. Beyond this angle, the light is totally reflected.

---

[3] The **critical angle** is the angle of incidence for which the angle of refraction is 90°. So TIR occurs.

Furthermore, it is necessary that light rays are sent inside the core with an angle minor the α_{max}, so that the light can propagate along the fiber, see figure 3 [9]:
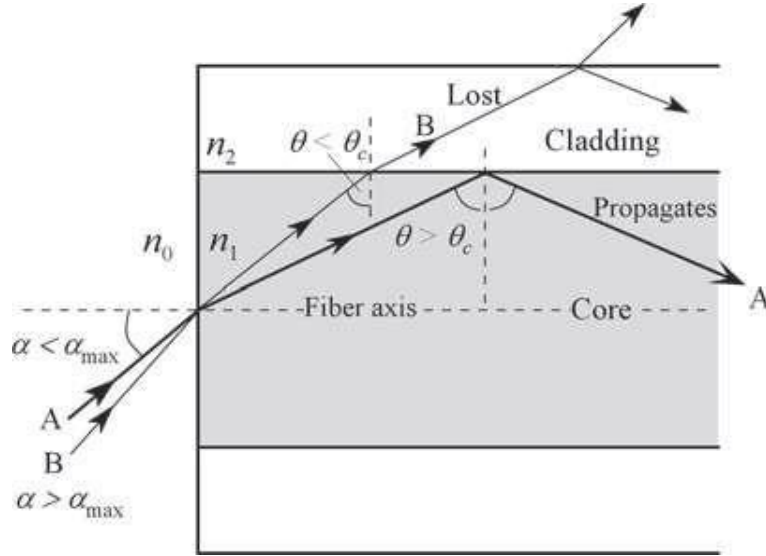
Figure 3: Characteristic Angles

The α_{max} indicated in figure 3 is the maximum acceptance angle [9]. This angle defines the range in which light can be sent inside the core for TIR takes place, instead beyond the highest acceptance angle, total reflection does not exist. It is possible to obtain α_{max} with the following steps.

To the interfaces between the core and external medium (generally the air), we can write:

$$n_0 \cdot \sin(\alpha) = n_1 \cdot \sin\left(\frac{\pi}{2} - \theta_c\right)$$

$$n_1 \cdot \sin(\theta_c) = n_2 \cdot \sin\left(\frac{\pi}{2}\right)$$

We Get:

$$\sin(\alpha_{max}) = \frac{(n_1^2 - n_2^2)^{\frac{1}{2}}}{n_0}$$

- n_1=refractive index of the core;
- n_2=refractive index of the cladding;
- n_0=refractive index of the external medium;
- NA is the numerator of the formulation above.

2.4 Advantages and Disadvantages of Optical Fibers

2.4.1 Advantages

- Low attenuation of signal. Especially in communication systems, it represents an important advantage because it permits to transmit the signal over a long distance. On the other hand, a common copper wire does not allow it.

- The fiber optics are transparent to the electromagnetic radiations and immune to lightning due to the optimum dielectric characteristics of the glass [3]. This advantage is important in Aeronautical and Space applications where is many electronic devices.

- Glass fiber optics, due to the high fusion temperature of the glass, are resistant to high temperatures. Moreover, glass is chemically stable, free from rust and resistant to corrosion, instead of the metal materials [3].
  These properties allow the use of fiber in almost every kind of harsh environment. Therefore, they can be used in environments which can catch fire or flammable, because of they do not create sparks [3].

- The material used is glass (silica) that is very abundant on the Earth instead of copper [3].

- The fiber optics are lighter in weight and smaller in size. Consequently, it permits to install fiber optics easily inside a structure: the reduction of the bulk reduce interference between structure and sensors. By considering a plastic coated fiber, the outer diameter is around 1 mm in respect of communication cable that has an outer diameter of 1 to 10 mm [3].

- The fiber optics are broadband and it allows sending and receiving a lot of information in high transmission speed.

2.4.2 Disadvantages

- The utilisation and maintenance of fiber optic is not cheap due to the high cost of many equipment required for fiber handling. For example, for the utilisation of FBG sensors it is necessary an expensive interrogation system and an expensive splicer is to splice two or more fibers.

- The fiber optics must be installed without small curve radius because of the increase of optical losses.

- During the installation high attention is needed because the fiber optic is susceptible to mechanical damage due to thin and susceptible structure.

3. Fiber Bragg Grating

In this case, the diffraction grating[4] [10] is achieved by means of a periodic variation of the fiber core index [1]. The periodic modulation is attained by means of a UV light laser, which locally modify the physics property of the material, increasing slightly the refraction index to printing a series of band in the core. This particularly structure is named *Fiber Bragg Grating* (FBG).
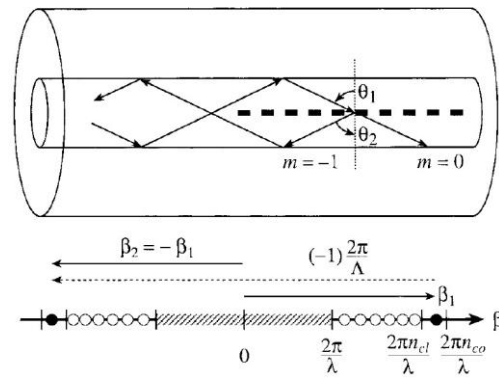
Figure 4: Reflection Grid

For the grid in the fiber is possible to determinate under what condition is verified a constructive interference for the transmitted light and reflected inside the fiber.
In the case of a wave, which propagates itself inside a means with an index of refraction *n* not unitary, the equation of maximum constructive interference become:

$$\Lambda n \, (sin\theta_2 - sin\theta_1) = m\lambda$$

Where Λ is the grid period. The effective refraction's index for both the corners become:

$$n_{eff_1} = nsin\theta_1$$

$$n_{eff_2} = nsin\theta_2$$

---

[4] **Diffraction Grating**: is an optical component with a periodic structure that splits and diffracts light into several beams travelling in different directions. The emerging coloration is a form of structural coloration. The directions of these beams depend on the spacing of the grating and the wavelength of the light so that the grating acts as the dispersive element.

And the propagation constant:

$$\beta_1 = n_{eff_1} \frac{2\pi}{\lambda}$$

$$\beta_2 = n_{eff_2} \frac{2\pi}{\lambda}$$

So, the equation become:

$$\beta_2 - \beta_1 = m \cdot \frac{2\pi}{\lambda}$$

In the optical fibers the first order of refraction is the most important, corresponding to m= -1.

The positive values of β, correspond to transmission mode while for the negative one is the reflection mode.

Depending on the direction in which are paired the modes, the gratings can be classified in *Bragg's Grating*, or reflection and transmission grid, also called *Long Period Gratings*.
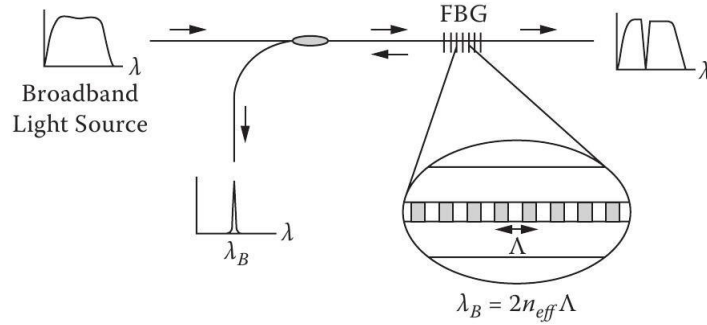
Figure 5: FBG Spectrum

Limited to the case of reflection grating, the reflection equation can be write:

$$\lambda = \Lambda(n_{eff_1} + n_{eff_2})$$

By demanding the transmission corner is the same of the reflection corner, so θ₁=-θ₂, we obtained the characteristic relation of a Bragg gratings, giving the wavelength λ_B corresponding the maximum reflected signal:

$$\lambda_B = 2n_{eff}\Lambda$$

The fact that the reflected wavelength depends on the grating path means that every variation is experienced the path could easily be detected like o wavelength variation.

For this reason, the Bragg's lattice could be used like sensors of deformation and temperature, also thanks to their slow invasiveness and facility to incorporating in the structure.

Another advantage is represented by the linearity of the dependence λ_B - Λ is maintained until the sensors breakage.

We have a strict translation inside the spectre only if we have a uniform variation of the grating path, condition that is verified when the sensor is subjective to a constant stress, mechanical or thermal.

If, for example, the sensor is acting on a variable deformation on the grating length, could change also the form of the spectre, making more complex or impossible the identification of the deformation.

With a linear deformation, however, the variation of the Bragg's wavelength gives the average deformation on the sensor.

The reflected power increases with the sensor's length, from the moment that also increase the number of reflections that the light experienced. In the same way, the longer sensors present a limited spectre.

3.1 Type of Grid

During the grid's inscription it is possible to modify even the optical characteristics that the geometrical one. In the first case we obtained apodizated grid which doesn't present lobes on the side of the principal spike.

In figure 6 is illustrated an apodization effect on the reflection spectre of a grid with the same characteristics.
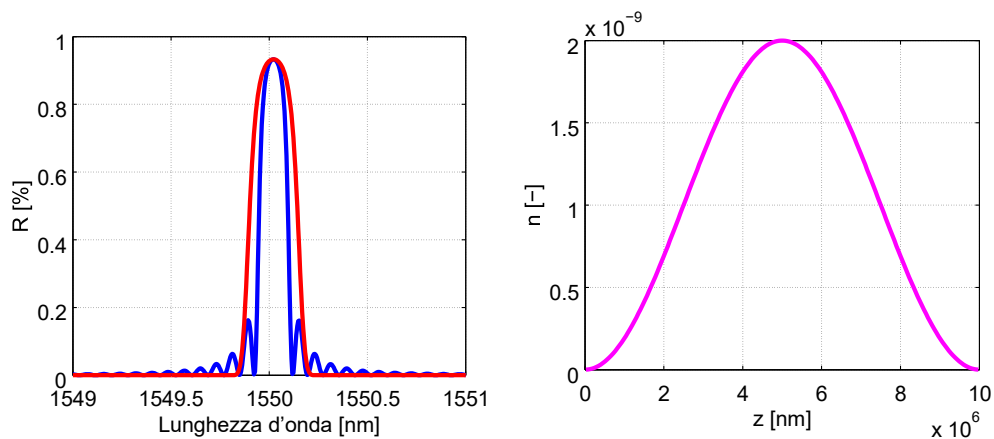
Figure 6: Reflection and Apodization Spectre

If the grating path of the is modified, *chirped* grating is obtained. This type of grids has a

larger spectrum: every fringe, having an Λ_i period different from the others, reflect a different wavelength λ_B. This characteristic can be used to any deformation with the arbitrary performance, as for it exists a relation between the wavelength and the position on the sensors [11].

The reconstruction of the deformation required some more complex proceedings, compared with the easy read of the variation of the spike's wavelength, from the moment that the information on the deformation's tree is contained in the specter's form.

3.2 Heat-Photo-Elastic Link

As already seen, a solicitation acting on the sensor it manifests itself by a variation in the reflected spectrum. To make this, the Heat-Photo-elastic link has been used, which bond the deformation with the variation of the optical propriety of a uniform grating.

The dependence of the variation of the wavelength variation from the variable to analyse.

$$\frac{\Delta \lambda_B}{\lambda_B} = \frac{\Delta \Lambda}{\Lambda} + \frac{\Delta n_{eff}}{n_{eff}} = \varepsilon_z + \frac{\Delta n_{eff}}{n_{eff}}$$

Where $\Delta \Lambda$ is the variation of the path which, divided for the unstrained grating, gives the deformation along the axis of the sensor axis ε_z while Δn_{eff} represent the variation of the refraction index of the grid due to the thermic or mechanical solicitation.

The axial deformation can be dissected to highlight the thermic and mechanical component.

$$\varepsilon_z = \varepsilon_z^t + \varepsilon_z^m = \alpha \Delta T + \varepsilon_z^m$$

Where α represents the thermic dilatation coefficient of the optical fiber.

Introducing the relation describing the variation of the refraction index, considering the elastic linear bond for the core of the fiber and using:

- **Photo-Elastic Constant** $p_e = \frac{n_{eff}^2}{2}\left(p_{12} - v(p_{11} + p_{12})\right)$
- **Termo-Optic Coefficient** $\zeta = \frac{1}{n_{eff}}\left(\frac{dn}{dT}\right)$

A compact form of the Photo-Termo-Elastic Link can be write, highlighting the dependence from the temperature of the mechanical solicitation:

$$\Delta \lambda_B = \lambda_B (1 - p_e)\varepsilon_z + \lambda(\alpha + \varsigma)\Delta T$$

Defining two new constant K_ε e K_T,

$$\Delta\lambda_B = K_\varepsilon\varepsilon_z + K_T\Delta T$$

The proportionality constants are experimentally determinate because often every sizes are not exactly known for the analytics' calculus [12] .

The discussion above is valid for the constant path grating but it could be applied on some short sessions of a chirped one, so that we wouldn't have meaningful modifications.

3.3 Production Technology: The Draw Tower Gratings

In a traditionally process of production, the fiber is initially spun and covered with the coating. The coating not permit the transition of the light so the portion destined to the inscription is treated to remove the coating (stripping) and after is exposed to a UV laser that locally modify the refraction index of fiber to inscribes the grating.

At the end of the process the part treated is covered with a new coating (recoting).

This method, used for the most part of sensors production, weakened the fiber in the point where the coating is removed, reducing the reliability of the sensors.

This problem is critical in the production of sensors array because the stripping and recoating area could be more extended, increasing the probability of a create fault.

The Draw Tower Gratings sensors are instead inscribed directly after the process of spinning of the fiber and before deposition of the coating, as illustrated in figure 7.
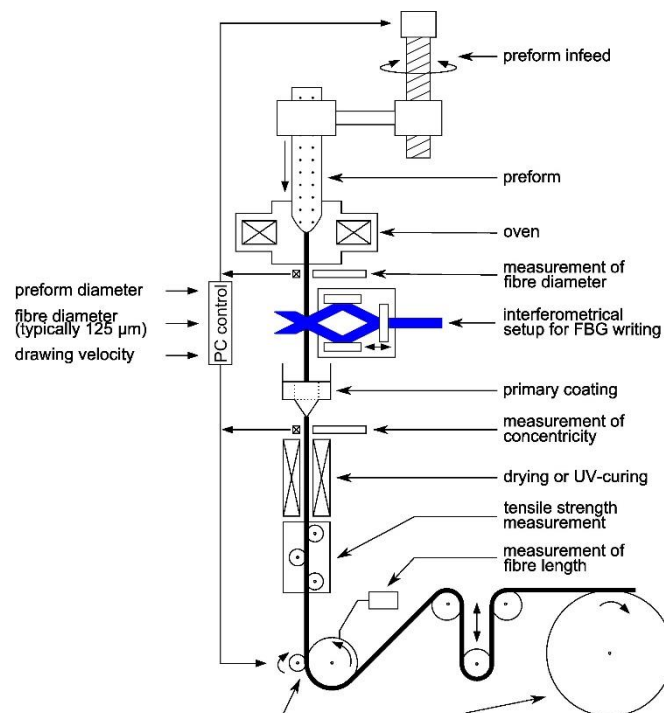
Figure 7: Draw Tower Gratings - Production

In this way the mechanical properties of the original fiber are kept.

In the past, the grating produced with this technique presented very low reflectivity, due to the exposure time limit due at high fiber spinning speed. In recent years, thanks to the use of materials with higher photosensitivity and better process control, which allows lower spinning speeds, it became possible to obtain gratings with reflectivity of 30-50% [13].

This innovative technology presents several advantages compared to a traditional production process:

- **High mechanical strength**: The coating is placed on the fiber after the grating inscription, so operations of stripping and recoating of traditional processes are unecessary. In this way the mechanical resistance of the sensor is up to 5 times greater of a traditional sensor.

- **Possibility of producing arrays of sensors**: this procedure allows to create easily very long arrays without discontinuity between a sensor and the next, and without glue more fibers in sequence (spliceless array).
  The minimum distance between the centres of two gratings, and therefore the spatial resolution of the sensor, is limited to 10mm due the spinning speed. Varying the length of the individual sensors and their wavelength it is possible to obtain spectra with characteristics different depending on the needs.

- **Low costs**: being a completely automatic process, the costs of arrays of sensors are relatively small, slightly higher to those of a single sensor obtained with traditional processes.

4. Theory for Mechanical Measurements

4.1 Basic Concepts

Almost every aspect of our life can be measured.

For example, if we want to know how many degrees are in our homes during winter's night we read the temperature on a thermostat. Direct use of this type of data, instruments and techniques are acquainted to us and the outcome doesn't need improved accuracy or other quantified methods.

However, this kind of data collection is insufficient in engineering research so it is necessary to pay attention in selecting the measurement equipment and techniques and in data analysis.

The objective in any measurement is to answer a question[14].

First of all, we need to define the concept of measurement: is the assignment of a number to a characteristic of an object or event, which can be compared with other objects or events [15]. In another way we can say the measurement is the act of assigning a specific value to a physical variable, called "measured variable".

Obviously, we need a Measurement System for quantifying the variables.

4.2 Measurement System

A measurement system *is a tool used for quantifying the measured variable and to extend the abilities of the human sense* [14]. It permits to give a specific value to sensed variables: human sense can recognize different degrees of a specific property of an object but are relative and not quantifiable.

A system is a set of components that work together to obtain a detailed result:

- **Sensor**: is *a physical element that employs some natural phenomenon to sense the variable being measured* [14]. To ensure high sensor accuracy and correct interpretation of data, passed by the system, high attention is required in sensor selection, installation and placement.

- **Transducer**: *convert the sensed information into a detectable signal* [14]. The output of a sensor needs a meaningfully form that can be recorded and the transducer is the component that does *only* this task. In fact, sometimes "transducer" means a subsystem composed by a sensor, a transducer and some signal conditioning elements. This definition allows us to avoid the ambiguity.

- **Output Stage**: *indicates or records the value measured*[14].

These are the main components of a system.

A **General Layout** for a measurement system can be described as follows in Figure 1.1 [14].
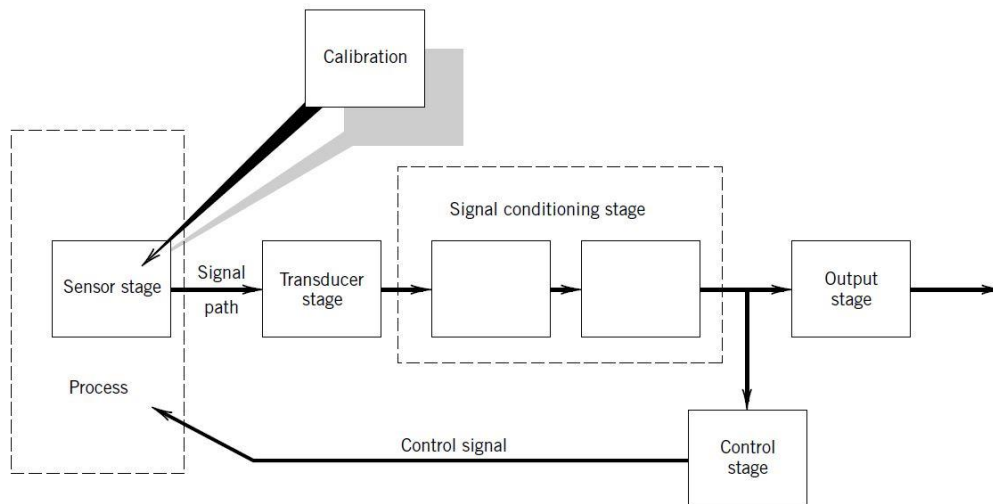
Figure 8: General Measurement System [1]

In the general layout the three *main* system's components, already mentioned, and two new *optional* elements can be seen:

- **Signal Condition Stage**: *takes the transducer signal and modifies it to a desired magnitude*[5] [14]. It has some different tasks such as providing linkage between the transducer and the output stage (optical or mechanical), cleaning signal using filtering techniques or using amplification systems to increase magnitude of signal.

- **Feedback – Control System**: it is made up of a controller that makes decisions about process control by interpreting the output signal. Its output is a signal that modifies the magnitude of the sensed variable by changing the relative process' parameters. For example, the control system can take decisions using magnitude comparison between outputs and high/low set points imposed by an operator.

---

[5] **Magnitude**: is the size of a mathematical object, a property which determines whether the object is larger or smaller than other objects of the same kind. More formally, an object's magnitude is the displayed result of an ordering (or ranking) of the class of objects to which it belongs. [20]

4.3 Test Plan

The aim of an experimental test is to answer just *one* question and that is why the variables that are going to be measured and also every other variable that can influence the output of the measurement system need to be known.

The existence of *secondary variables* is an issue carefully considered in designing test plans because gathering data can be highly affected by these ones and they can prevent reaching an accurate measurement.

Also, the accuracy of the answer is a factor strictly connected to these variables beyond the primary ones: higher precision required needs much restricted controls.

The ability to counteract the effects of secondary variables derives from the capability to conceptualise test's influencing factors and plan the test around these.

As it can be seen later, in our test plan there are some external influencing factors challenging us like rubber softness in the fiber locking systems, vibration from the ground and room air circulation, the effect of gravity on long suspended fibers and no-homogenous thermal distribution around the Fiber Bragg Grating[6] (FBG) sensor.

The Steps for a test plan are:

1. **Parameter Design Plan**: *determine the test objective and identify the process variables and parameters and a means for their control* [14].
2. **System and Tolerance Design Plan**: *select a measurement technique, equipment and test procedure based on some preconceived tolerance limits for error* [14].
3. **Data Reduction Design Plan**: *plan how to analyse, present and use the anticipated data* [14]*.

4.4 Element of an Experimental Test Plan

4.4.1 Variables

A Variable is an element that can change the test. In fact, analysing her etymology, it's noticeable that it comes from Latin *variabilis*, which means "capable of changing".

Using **Cause-and-Effect** relationship, variables can be separated in:

- ▪ **Independent Variable**: can change in significant way without any effect on the value of other variables.
- ▪ **Dependent Variable**: is affected by changes in other variables.

Both independent and dependent variables may be discrete if they can be quantified in a

---

[6] **FBG**: is a type of distributed Bragg reflector constructed in a short segment of optical fiber that reflects wavelengths of light and transmits all others. This is achieved by creating a periodic variation in the refractive index of the fiber core, which generates a wavelength-specific dielectric mirror. [21]

discrete way or continuous if their value can change in a continuous way.

The cause-effect relationship between variables merges from the **control** of variables themselves. Defining the control as the ability to hold a variable at a predetermined value, the dependent variable can be measured by controlling the independent value.

Unfortunately, some variables that affect the measurement cannot be controlled during the process: they are called **extraneous variables**. This type of variables introduces false information and modifies the behaviour of that variable confusing the cause-effect relation of the measurement.

4.4.2 Parameters

We define a ***parameter*** *as a functional grouping of variable*[14].

If a parameter can modify the value of a measured variable then it is a *control parameter* while it is a *controlled parameter* if its value can be monitored during the measurement.

4.4.3 Noise and Interference

- **Noise**: *is a random variation of the value of the measured signal as a consequence of the variation of extraneous variables*[14]. Better signal information is taken by using statistical techniques.
- **Interference**: *impose a undesirable deterministic trend on the measured value*[14]*.* False trend reduction is the most important action that must be taken, so the trends need to be "transformed" into random variation in the data set even if this increases the scatter in the measured value. Randomization methods are available and can be easily incorporated.

4.4.4 Randomization

The test plan randomization depends on the type of variable in analysis.

The following chapters will show how our test bench gives the opportunity to carry out both discrete and continuous measurement so we need to create different random tests.

The first step in the test plan involves only discrete variables. The output of this kind of measurement can be affected by some extraneous variables such as different test operators, different test operating conditions and the use of different instruments. The randomization, to minimize discrete influences, can be done using random block. A block is a data set of the measured variable where the extraneous variable is fixed.

Next step includes continuous variable which is randomized by using a casual order of the independent variable. This way the coupling between slow and uncontrolled variation in the extraneous variables and its applications in the value of the independent variable is broken.

4.4.5 Replication and Repetition

The increase in precision is achieved by using a higher number of measures.

- **Replication**: *is an independent duplication of a set of measurements using similar operating conditions*[14]. Replication, evaluating the variation in the measured variable in the tests, allows to reset the conditions of the desired value. So, it is possible to have the control over the operating conditions and the procedure. This is a "big Up" compared to a simple repetition.

- **Repetition**: *are repeated measurements made during any single test run while the operating conditions are held under control* [14].

4.5 Calibration[7]

First of all, a **static** calibration of the system is needed. This is the most common type of calibration procedure where only the magnitude of input and output are remarkable and the values of the variable involved remain constant.

Direct calibration curve is obtained applying a range of input values (usually a controlled independent variable) and by observing the output (dependent variable of calibration). This represents the interpretation logic – I/O relationship – for the measurement.

A calibration curve can be also used in creating a correlation: a function I/O relationship will have the form $y = f(x)$ determined using curve fitting techniques.

The slope of the static calibration curve represents the static sensitivity K which indicates the change of the output associated with a change in the input.
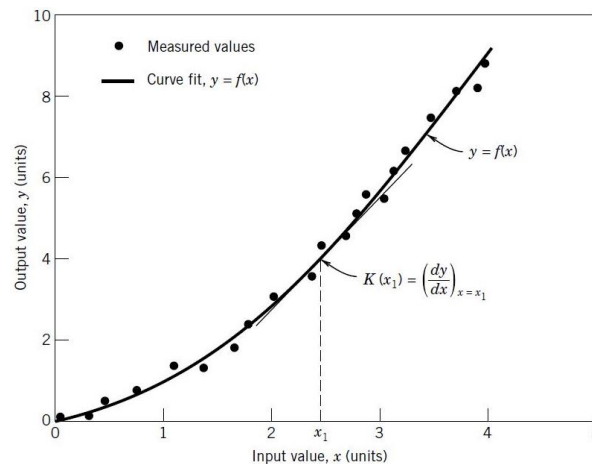
Figure 9: Static Calibration Curve [1]

---

[7] **Calibration**: Operation that, under specified conditions, in the first step, establishes a relation between the quantity values with measurement uncertainties provided by the measurement standards and corresponding indications with associated measurement uncertainties (of the calibrated instrument or secondary standard) and, in the second step, uses this information to establish a relation for obtaining a measurement result from an indication [4].

4.5.1 Range

The range define the operating limits of the system, that are from the minimum to the maximum values used in the measurement system.

- **Input Range**: is defined as extending from x_{min} to x_{max}.
- **Output Range**: is defined as extending from y_{min} to y_{max}. The Full-Scale Operating Range (FSO) is:

$$r_0 = y_{max} - y_{min}$$

4.5.2 Accuracy and Error

The accuracy is the "*closeness of agreement between a measured quantity value and a true quantity value measured*"[15].

A *true value* is defined as the exact value of a variable but rarely this value can be exactly known because some errors influence it. Even the measured value is affected by error: so, the concept of accuracy of a measurement is a qualitative one.

From accuracy definition we can express the *error* (it is important to note that this is only a reference definition) as:

$$e = Measured\ Value - True\ Value$$

Sometimes the error estimation is based on a surrogate reference value used in the calibration phase. The *relative error* is:

$$A = \frac{|e|}{Ref.Value} x100$$

4.5.3 Uncertainty

It is called uncertainty the *numerical estimate of the possible range of the error in a measurement*.

Error in any measurement is unknown because the true value is rarely known, so a strictly definition of uncertainty introduces a probabilistic approach: the uncertainty becomes the interval around the true value in which the measured value is found with a stated probability.

First, an uncertainty is assigned based on the available information which allows the error to be restricted within certain limits.

It is evident that uncertainty is inherent in any system error and is a property of the test result: it represents a powerful tool to quantify the quality of the result to allow evaluating measurement system and test plan efficiency.

The assignment of an uncertainty value to the measurement system takes place through

the analysis of the interaction between the random and systematic errors, affecting the system itself, the calibration procedure and the standard used.

4.5.4 Errors Classification

Errors are properties of the single components of the measurement system. They involve each test phase and hide the true value of a variable.

Errors can be divided into two types:

- **Random Errors**: under fixed operating conditions, random errors appear as scatter of the measured data. They are inherent the resolution and the repeatability capacity of the system, the procedure, the calibration, the temporal and spatial variation of variables and the variation in the operative and environmental conditions of the process.

- **Systematic Errors**: under fixed operating conditions, they are constant during repeated measurements and are a cause of an offset in the estimation of the true value.

  Their main characteristic is the "constancy": for this reason, they are harder to detect than random errors. An example of systematic error is to measure a person's height while wearing shoes.

  Observing these errors is a challenge to which can be responded introducing several detection methods:

  1. Calibration: using a standard, instrumental systematic errors can be reduced in a predictable interval. It is also possible to use high quality instruments with a calibration certificate.
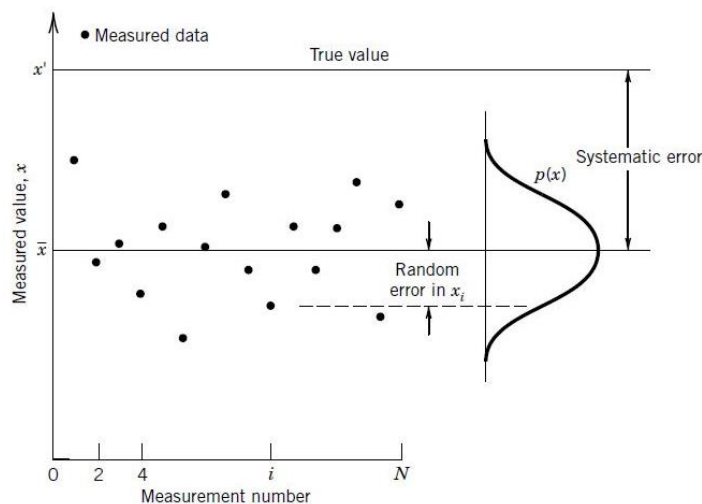
Figure 10: Distribution of Random and Systematic Errors [1]

35

2. Concomitant Methodology: the test plan can include different methods to measure the same thing, preferably using different physical way to obtain the results.
3. Interlaboratory Comparisons: it is possible to check the result with other laboratory (that means other different environmental condition, instruments, facilities but similar measurement procedure) to have a statistical estimate of the systematic uncertainty.

It is important to notice that using high-quality instruments, we accept the hypothesis of no systematic error on our test bench [1].

4.5.5 Error Sources

Identification of the error sources pass through the analysis of the staging of the measurement process. We can design the process in three stages, which one has its error sources.

- **Calibration Errors**: although it may seem paradoxical, the error analysis suitable for the calibration of the measurement system must provide for the analysis of the errors of the calibration itself. They come mainly from three sources:
    1. Reference Value used in calibration
    2. Instruments
    3. Process
- **Data Acquisition Errors**: are errors appeared during the measurement. Common sources are:
    1. Unaccounted sensor errors
    2. System operating condition changing
    3. Installation effects on sensors
- **Data Reduction Errors**: are "mathematical" errors like curve fits, correlation, truncation, interpolation and errors from assumed models.

4.5.6 Design-Stage Uncertainty Analysis

The design-stage uncertainty analysis is an analysis made prior to any test and provide a first estimate of the minimum uncertainty reached with the select instruments and method set-up. Obviously, if the value obtained is unacceptable, alternate approach will be found.

So, the analysis is useful for instruments and measurement techniques selection based on their relative performances.

During this phase, there isn't distinction between systematic and random errors and we

take in account two individual contribute to uncertainty which allows us to determine the "global" uncertainty u_d:

$$u_d = \sqrt{(u_0)^2 + (u_c)^2}$$

where u_0 is the *zero-order uncertainty* and u_c is the *instrument uncertainty.*
Let's now evaluate the individual contributions:

- **Zero-Order Uncertainty u_0**: *is an estimate of the expected random uncertainty caused by data scatter due to instrument resolution while all other aspects of the measurement are perfectly controlled. Missing other information, assign a numerical value of one half of resolution or to its digital least count reasonably represent the uncertain interval with a probability of 95%* [14].

$$u_0 = \pm\frac{1}{2} * resolution = 1 \; Last \; Significant \; Digit \; (LSD)$$

   As explained below in the statistical analysis the ± come from the assumption of a normal distribution for the error.
- **Instrument Uncertainty u_c**: *is an estimate of the expected systematic uncertainty due to the instruments* [14].
   Often this error is delineated into parts and need to be combinate. To accomplish the task, we used the Root-Sum-Squares (RSS) Method.

4.5.7 Root-Sum-Squares [RSS] Method

The RSS is a statistical analysis method able to evaluate the *uncertainty propagation[8].* The method is based on the idea that the square of an uncertainty is a measure of an error's variance and its propagation yields an estimate of the total uncertainty. The engineers commonly report the final uncertainty at a 95% probability level, equal to the probability of two standard deviation (as we will see during the statistical analysis).
The uncertainty of the measured variable u_x estimate with the RSS method is:

$$u_x = \sqrt{\sum_{K=1}^{K} (u_k)^2}$$

Where K is the number of errors.

---

[8] **Uncertainty Propagation**: is the effect of variables' uncertainties on the uncertainty of a function based on them. When the variables are the values of experimental measurements they have uncertainties due to measurement limitations (e.g., instrument precision) which propagate due to the combination of variables in the function [3].

4.5.8 Type of Random Error

- **Hysteresis (u_h)**: is about the difference between up/downscale sequential test. It occurs when the output of a measurement is dependent on the previous value indicated by the system. Usually the hysteresis error is indicated as a percentage of the full-scale output range r_0.

$$\% u_{h_{max}} = \frac{u_{h_{max}}}{r_0} \, x \, 100$$
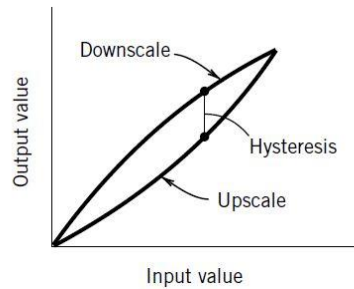
Figure 11: Hystereris Error [1]

- **Linearity Error (u_L)**: describe the nonlinear behaviour of the real system respect of the linear relationship of the measurement device specification.

$$u_L(x) = y(x) - y_L(x)$$

Like the hysteresis error, the nonlinear behaviour is described in terms of the maximum linearity error as a percentage of the full-scale range.

$$\% u_{L_{max}} = \frac{u_{L_{max}}}{r_0} x \, 100$$
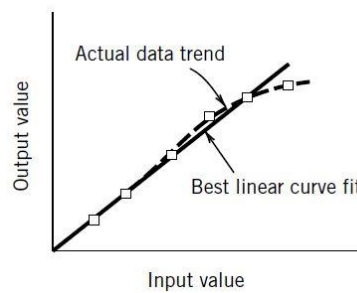
Figure 12: Linearity Error [1]

- **Sensitivity (u_K)**: is a statistical measure of the random error in the estimate of the slope of the calibration curve.

- **Zero Error (u_z)**: If the sensitivity is constant but the zero intercept is not fixed we can see a vertical shift of the curve, that is the zero error. This error can be reduced with periodically adjusting. During our experience the zero error has emerged in hard and soft rubber analysis in which fiber strain preloading has modify our measurements.
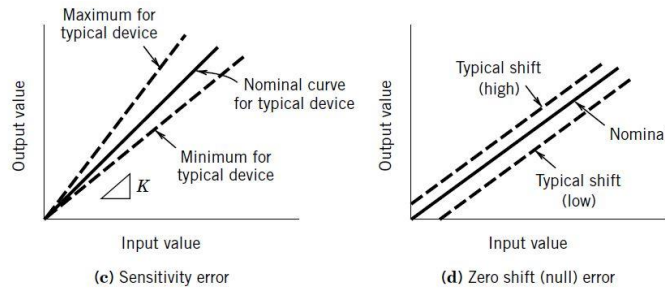
Figure 13: Sensitivity and Zero Errors [1]

- **Repeatability (u_R)**: is the ability of a measurement system to indicate the same value in different and independent application.

$$\% u_{R_{max}} = \frac{2 s_X}{r_0} * 100$$

Where s_x is the standard variation.

4.6 Statistical Measurement Analysis

As previously said, our analysis accepts the "*No Systematic Errors*" hypothesis and even if they are present, they do not vary from one measurement to the other and do not change the statistical analysis: so, we need only a statistical support for the study of random errors.

We can estimate the true value x' as:

$$x' = \bar{x} \pm u_{\bar{x}}$$

Where $\bar{x}$ is the calculated simple mean (represent the most probable estimate of x' based on available data) and $\pm u_{\bar{x}}$ is the uncertainty interval.

As all engineering research, data sets are finite-sized and require the use of appropriate statistical methods. Define N as the number of data points, we can see if N is small, the estimation of x' is strictly connected to all data point; while, if N tends to infinite, all the possibility is included in data sets.

4.6.1 Probability Density Function [PDF]

The frequency with which the measured variable assumes a particular value or interval of values is described by its Probability Density [14].

Analysing data point of each measurements of a variable and plotting the value on an axis we note that the points be disposed within some interval around one preferred value. *This tendency toward one central value about which all the other values are scattered is known as a central tendency of a random variable*[14]. We can use the probability density to determine the central value and the scattered about it: finding the interval where data point tend to clump, we might expect that the true mean value of x is somewhere in the clump.

It is possible to create a Histogram to show the tendency and the probability density of a variable. This chart is created by dividing the abscissa axis (which contain values from minimum to maximum of the measured values) in K small intervals and plotting on the ordinate the number of times n_j that the measured value assumes a value within a x_k interval.

Furthermore, nondimensionalizing the number of times using number of data set point to obtain a frequency, the histogram can be converting into a frequency distribution.

A definition of K is needed. A solution for K estimation is given in the Bendat and Piersol [16]:

$$K = 1.87(N-1)^{0,4} + 1$$

We work with small N, so the number of K should be chosen with a simple rule that $n_j > 5$ for at least one interval.

If N→∞, the probability density function becomes:

$$p(x) = \lim_{\delta x \to 0} \frac{n_j}{N(2\delta x)}$$

The probability density function defines the probability that a measured variable might assume a particular value upon any individual measurement. It also provides the central tendency of the variable and its variation. This central tendency is the desired representative value that gives the best estimate of the true mean value[14].

The nature of variable and the environment around the process are fundamental elements in definition of the shape of probability density function. Often the overall shape looks like a standard distribution: using the histogram we can "override" the need to have very large N to find the distribution suitable for our data.

Plotting the data at our disposal, we observed a correspondence between the histogram and the Gaussian distribution which has become the milestone for our statistical analysis.

4.6.2 Finite-Sized Data Sets Analysis

N is not infinite: we must use a *Finite Statistics* approach, which is able to describe only the behaviour of considered data set.

The result coming from the use of Finite Statistic are reliable and used without comparison with the actual probability density function. They are:

1. **Sample Mean Value $\bar{x}$**: indicate the probable value of the true mean value, x'.

$$\bar{x} = \frac{1}{N} \sum_{i=1}^{N} x_i$$

2. **Sample Variance s_x^2**: represent a probable measure of the variation in the data set.

$$s_x^2 = \frac{1}{N-1} \sum_{i=1}^{N} (x_i - \bar{x})^2$$

3. **Sample Standard Deviation s_x**:

$$s_x = \sqrt{s_x^2} = \left(\frac{1}{N-1} \sum_{i=1}^{N} (x_i - \bar{x})^2 \right)^{\frac{1}{2}}$$

Where $(x_i - \bar{x})$ is the deviation of x_i.

Finite data sets do not provide a real weight estimate of the true probability like the p(x). To solve this problem a coverage factor for finite data set is introduced in the definition of the single measurement:

$$x_i = \bar{x} \pm t_{v,P} * s_x$$

Where $\pm t_{v,P} * s_x$ is the interval within which any measurement value is at a given probability.

The coverage factor is referred to the *Student's t variable*.

$$t = \frac{\bar{x} - x'}{s_x / \sqrt{N}}$$

The *Student's t Distribution* was developed by William S.Gosset [17] in the 1908 with the alias of "student" because the Guinness brewery in which it was employed forbade its employees to publish articles so that they would not divulge production secrets.

The value of t is tabulated in function of the probability P desired and the degrees of freedom v=N-1. Observing Table 1, we highlight the fact that t increases the size of the interval required to obtain the desired percentage. Obviously, increasing N, t value matches the interval given by a normal distribution as we can see in Figure 7.
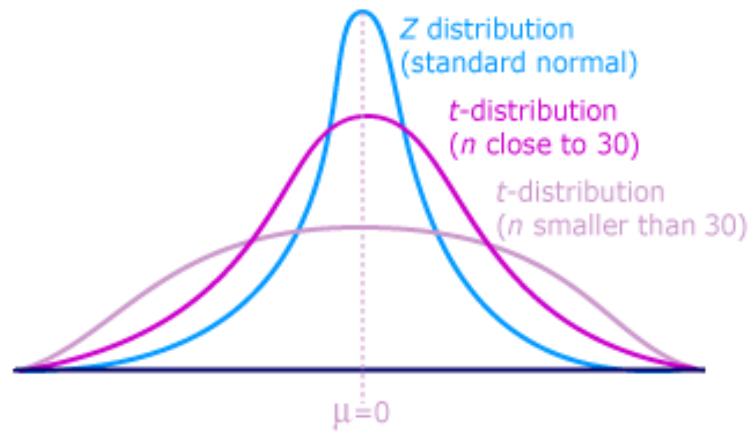
Figure 14: Comparison between Standard and t-modify Normal Distribution

ν	t_{50}	t_{90}	t_{95}	t_{99}
1	1.000	6.314	12.706	63.657
2	0.816	2.920	4.303	9.925
3	0.765	2.353	3.182	5.841
4	0.741	2.132	2.770	4.604
5	0.727	2.015	2.571	4.032
6	0.718	1.943	2.447	3.707
7	0.711	1.895	2.365	3.499
8	0.706	1.860	2.306	3.355
9	0.703	1.833	2.262	3.250
10	0.700	1.812	2.228	3.169
11	0.697	1.796	2.201	3.106
12	0.695	1.782	2.179	3.055
13	0.694	1.771	2.160	3.012
14	0.692	1.761	2.145	2.977
15	0.691	1.753	2.131	2.947
16	0.690	1.746	2.120	2.921
17	0.689	1.740	2.110	2.898
18	0.688	1.734	2.101	2.878
19	0.688	1.729	2.093	2.861
20	0.687	1.725	2.086	2.845
21	0.686	1.721	2.080	2.831
30	0.683	1.697	2.042	2.750
40	0.681	1.684	2.021	2.704
50	0.680	1.679	2.010	2.679
60	0.679	1.671	2.000	2.660
∞	0.674	1.645	1.960	2.576

Table 1: Student's t Distribution [1]

4.6.3 Standard Deviation of the Means

Small sample sets tend to have different statistic than the entire sample from they come from is a big problem for finite data sets.

Computing a set of mean value using M replication of N measurement is possible to see that this mean value be Gauss-distributed around a central value.

Variation in the sample means are linked with the sample variance and the sample size and is characterized by a normal distribution around the true mean.

With a single finite data set it is possible to evaluate the variance of the distribution of mean value using the *standard deviation of the means*:

$$s_{\bar{x}} = \frac{s_x}{\sqrt{N}}$$

The standard deviation of the means represents a measure of how well a measured mean represents the mean of the population [14]. It is a property of the data and show how the mean can be distributed about a true mean value.

So, the true main value of finite data set is:

$$x' = \bar{x} \pm t_{v,P} s_{\bar{x}}$$

Where $\pm t_{v,P} s_{\bar{x}}$ is the *confidence interval:* a quantified measure of the random error in true value estimation at an assigned probability, indicated by t. $s_{\bar{x}}$ is the random standard uncertainty and $t_{v,P} s_{\bar{x}}$ indicates the random uncertainty in the mean value at P% confidence.

4.7 Selected Strategy

This chapter provides the guidance lines for a complete statistical analysis of data gather from experimental measurement that will be useful for our "successor".

The starting goal of our team is the construction of the test bench for the mechanical and thermal characterization of FBG sensor.

But, even if obtaining the right instrumentation in a reasonable amount of time was a big challenge due to intricate bureaucracy that afflict our university, we succeeded in a shorter time than expected and we decided to try a first characterization of the system in a simplified way but adapted to the time available to us.

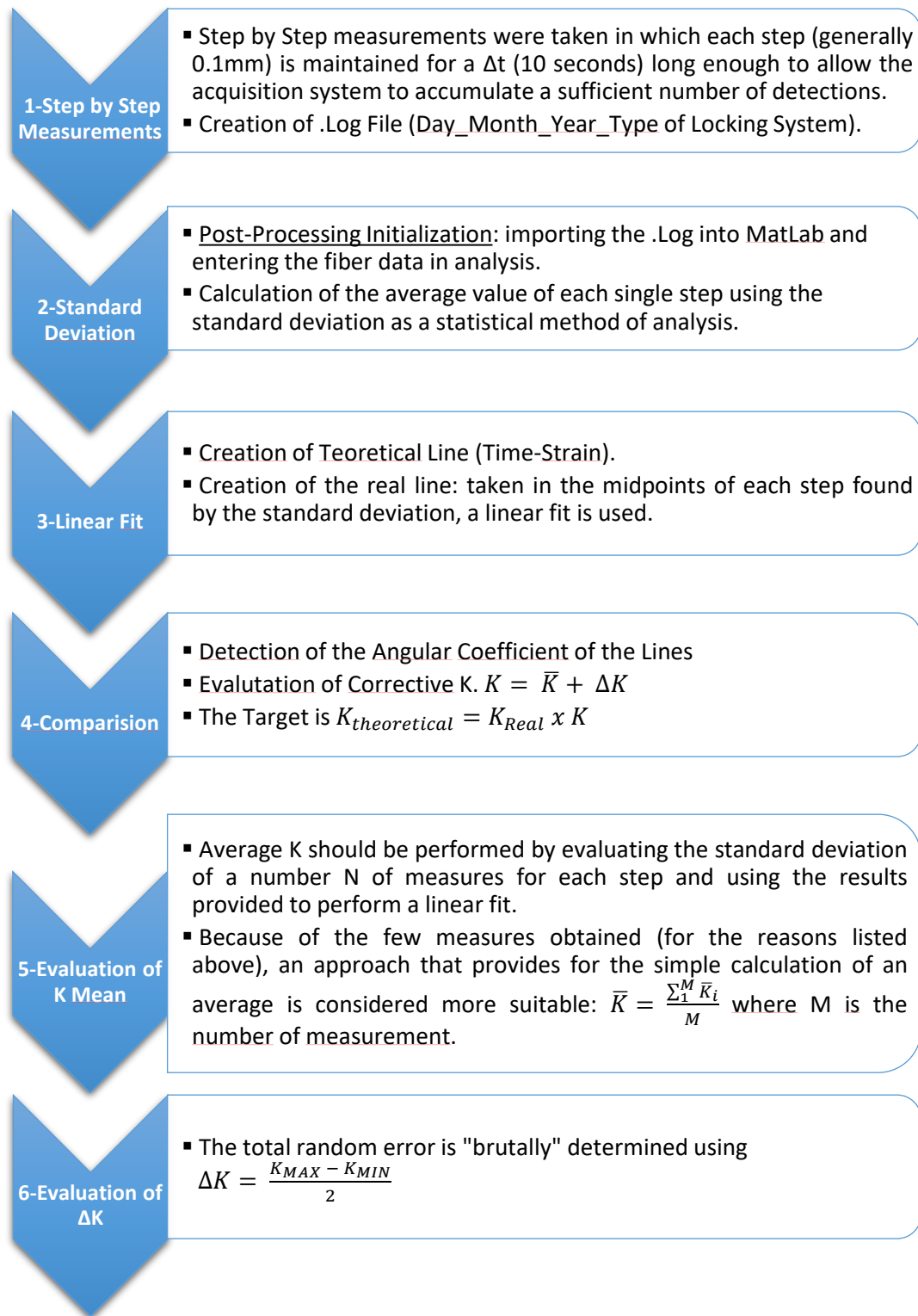The choices are show in the flow chart below, in figure 8.

1-Step by Step Measurements
- Step by Step measurements were taken in which each step (generally 0.1mm) is maintained for a Δt (10 seconds) long enough to allow the acquisition system to accumulate a sufficient number of detections.
- Creation of .Log File (Day_Month_Year_Type of Locking System).

2-Standard Deviation
- Post-Processing Initialization: importing the .Log into MatLab and entering the fiber data in analysis.
- Calculation of the average value of each single step using the standard deviation as a statistical method of analysis.

3-Linear Fit
- Creation of Teoretical Line (Time-Strain).
- Creation of the real line: taken in the midpoints of each step found by the standard deviation, a linear fit is used.

4-Comparision
- Detection of the Angular Coefficient of the Lines
- Evalutation of Corrective K. $K = \bar{K} + \Delta K$
- The Target is $K_{theoretical} = K_{Real} \, x \, K$

5-Evaluation of K Mean
- Average K should be performed by evaluating the standard deviation of a number N of measures for each step and using the results provided to perform a linear fit.
- Because of the few measures obtained (for the reasons listed above), an approach that provides for the simple calculation of an average is considered more suitable: $\bar{K} = \frac{\sum_1^M \bar{K}_i}{M}$ where M is the number of measurement.

6-Evaluation of ΔK
- The total random error is "brutally" determined using $\Delta K = \frac{K_{MAX} - K_{MIN}}{2}$

Figure 15: FBG Characterization Strategy

The chart in Figure 8 show the logical and practical approach follow in our characterization attempt but some clarifications are needed:

1. Step by Step Measurements: for each hypothetical situation, several measures have been carried out. Different kind of locking system (Soft Rubber, Hard Rubber, Epoxy Glue, Araldite 2021©) and different length, see as the distance between the locking system with the FBG in the middle of the line, are used to simulate changed application. Long Δt is used to tame the high sensibility of sensors. As will be explained later in fact, the workbench is designing to mitigate noise effect such as ground vibration (absorbed by a pneumatic anti-vibration table in collaboration with passive Sorbothane feet) and atmospheric air circulation in the Lab (moderate by a plexiglass box).

2. Standard Deviation: the statistical analysis is used to elaborate the bench mitigate-data but also for evaluate, as we see below, the scattering of manual imput of translation stage. The concept is illustrated in Figure 9 below.
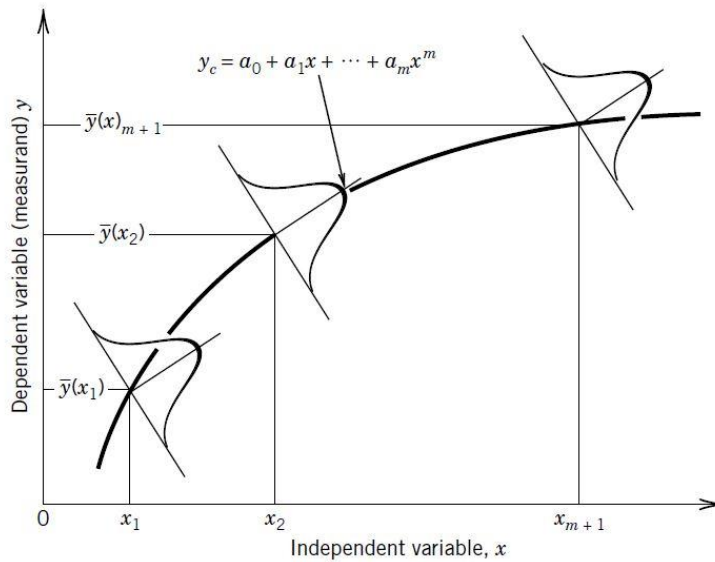

Figure 16: Concept of Standard Deviation Use [1]

3. Linear Fit: the fit, using Matrix Laboratory (MatLab) integrated function *polyfit*, is evaluate with the Ordinary Last Square (OLS) Method.

4. Comparison: is important to underline the dependence of components of K. In particular $\overline{K}$ is function of stretchiness of some of system elements like fiber core, fiber coating, rubber/glue and locking system and in function of line length L_0.
   While ΔK is function of instruments (gauge and linear actuator – translation stage).

As previously said, in chapter 5.5.5, it is necessary to evaluate also the Calibration Errors. Mainly, the most important error source is the manual imput of the translation stage, the Optosigma TADC-401C.

To estimate the quality and the accuracy of the imput, we need to find the Repeatability Error, defined in the chapter 5.5.8:

$$\%u_{R_{max}} = \frac{2s_X}{r_0} * 100$$

Obviously, it is necessary have some measurement for obtain an acceptable output of standard deviation.

It may seem contradictory, but to get these measurements was used using the same FBG sensors that our system must characterize.

This is possible because there is a huge difference in sensitivity between the instruments: the linear actuator has a resolution of 0.01 mm (10^{-5} m) while an FBG sensor has a much higher precision, in the order of 10^{-9} m.

This difference makes it possible to have a first estimate of the accuracy of the input supplied, although still affected by system errors (which are in any case much lower than 10^4) and of common measurement errors such as parallax.

In addition to error is important to check the "form" of the imput scattering. In fact, is fundamental data scattering is random with any kind of progressivity. The progressivity is an evidence of slip of the fiber or of the locking system while a small dispersion is equivalent a very little strain variation.

5. Assembly of Test Bench

To achieve the goal of test and validate the FBG sensors a test bench was assembled. The chapter explain the design process and the solution adopted to solve critical issues merged during the design phase and during the "manufacturing" phase.

Obviously, being a totally innovative experimental research, a "search and destroy" approach was sometimes used.

5.1 Platform

The facility is constituted by two breadboards mounted on a pneumatic anti-vibration table.

The *thermal* breadboard is equipped with locking system and a "thermal unit" composed by an aluminium conductive structure where a PT100 sensor and a Peltier Cell, connected with a controller, are installed.

The *strain* breadboard, which a greater attention has been dedicated, has a standard layout with four testing lines which one is a composition of a "translation unit" consisting of an adapter, a micro-translation (Optosigma TADC-401) stage and a locking system and a static locking system at the other side of the line. Every "line" can have different length: so, we can characterize different situation directly linked to different fiber application. Obviously the fiber optic is brim between the two-locking unit.

The facility is completed with the interrogation system, explained in detail in the next chapter, and a computer.

Initially, the breadboard was mounted on a wood platform equipped with a case to protect the instruments from accidental touch that can cause fiber breakage.

This was the first time to adopt the "search and destroy" approach: the initial test on the board underline big problems due to ground vibration. The measurements were strongly susceptible to vibrations.

In fact, the FBG sensor has a characteristic *Center Wavelength* called *Bragg Wavelength* λ_B that shifts in response to strain or temperature variations. So, vibration causes an additional shift of λ_B, by reducing the accuracy of measurements.

For this reason, a combination of three solutions were adopted:

1. Elimination of Wood Platform and Box;
2. Breadboards positioned on an Anti-Vibration Table;
3. Installation of Passive Dumper under the strain breadboard.

The chosen dumpers are the *Thorlabs AV4* Passive Dumper. They are made of Sorbothane[9] [18]. In figure 10 is show the load-frequency graph. The estimate total weight of system is around 20 Kg, so each of them has a load of about 5 kg. Notice the dumpers are loaded almost to the limit: in this way they absorb a wide range of frequency as desired due to inability to detect the ground vibration frequency.
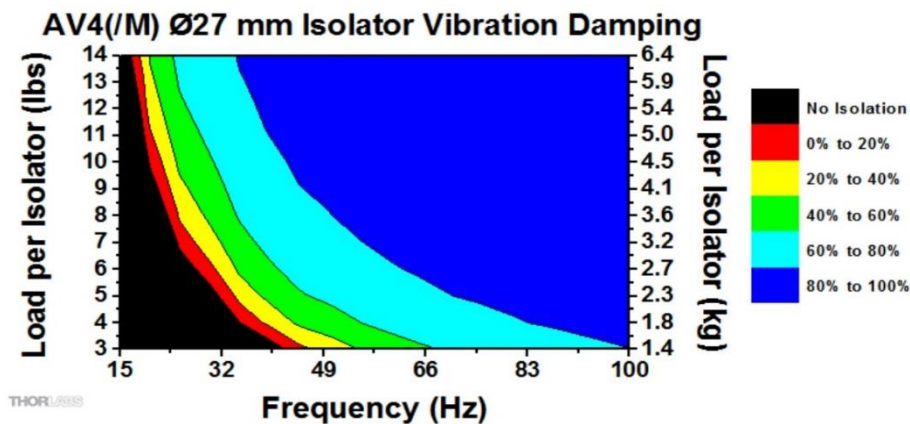

Figure 17: Load Frequency of Passive Dumper [Copyright 1999-2018 Thorlabs, Inc.]

The updated made on the system improve accuracy of the measurement but, for strain measurement, as already said in chapter 6, another source of vibration "annoy" the system: room air circulation. The solution applied to solve this issue is the use *Thorlabs XE25C10D/M Enclosures* properly adapted for our task (four holes were made to allow fiber-interrogator connection).

Figure 18: Plexiglass Case [Copyright 1999-2010 Thorlabs, Inc.]

---

[9] **Sorbothane** is the brand name of a synthetic viscoelastic urethane polymer used as a shock absorber and vibration damper. It is manufactured by Sorbothane, Inc., based in Kent, Ohio.
The material combines some of the properties of rubber, silicone, and other elastic polymers. It is a good vibration damping material, an acoustic insulator, and highly durable.
Sorbothane is a visco-elastic material, meaning that it exhibits properties of both liquids (viscous solutions) and solids (elastic materials), with a relaxation time of two seconds [5].

5.2 Locking System for Mechanical Testing

5.2.1 Aluminium Locking System

The locking systems were designed making CAD models with *SolidWorks*, a Dassault Systemes software.

The locking system for mechanical testing is consist of three main components:

1. Upper Base
2. Lock Section
3. Bottom Base

Obviously, the locking system is built with the aim to permit the catch of the fiber between the two bases. The "lock section" is necessary to avoid fiber crushing. In fact, the closure of the upper plate was designed with six screws to permit to apply a load. Notwithstanding, even if a "controlled" and uniform load was applied, a strain variation causing fiber crushing appeared. So, insert a medium between fiber and locking components become fundamental. Several tests with different middle layer such as double side tape led to the choice of the rubbers as the best solution.

Rubber selection is another critical point of locking design process because the rubber's stiffness influences severely the measurement in two ways: the rubber can slide away from the lock box and has an own deformation under a normal load.

During these tests some fiber broke up due rubber flattening: the necessary load to block the fiber gives a deformation in the rubber in the unload system. The deformation generates a shear stress that damages up to break the fiber, as show in figure 10. To counteract this inconvenience, it is important to cut accurately the rubber to be sure to avoid this phenomenon.

Figure 19: Rubber Flattening

The bottom component is mounted on the microtranslation stage and to facilitate the connection has the same size.

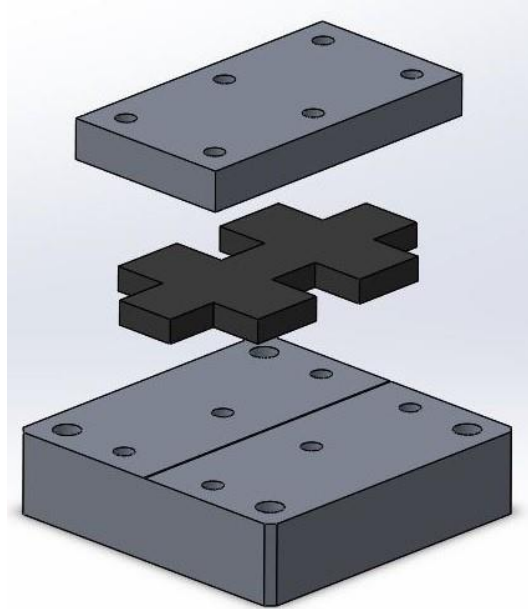The exploded view drawing is show in figure 13.

Figure 20: Exploded View of Strain Locking System 1

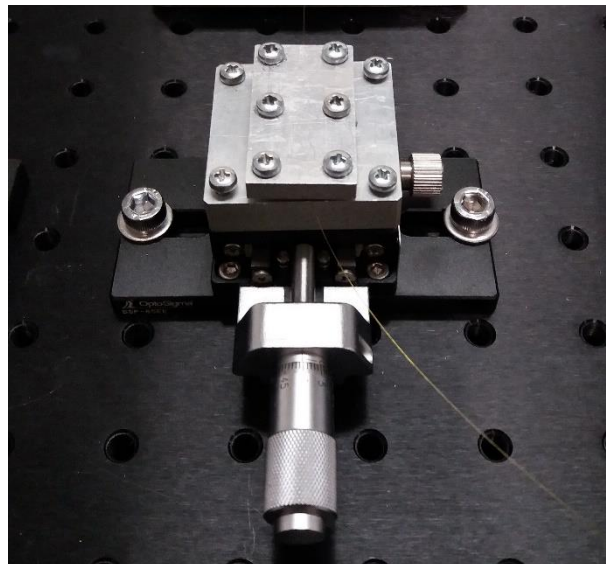In Figure 14, below, the manufactured product is show:

Figure 21: Locking System 1 - Manufactured

It is possible to notice that the microtraslation stage is not directly mounted on the breadboard. Different manufacturer uses different standards and so the mounting holes are not suitable with the holes of the board. An adaptor was installed to solve this problem. The adaptor purchase iter cause a loss of two weeks of analysis.

Second locking system is quite similar to the first, but it has not the translation stage. The upper plate is the same of the other locking system, to speed up production and reduce cost.

The bottom base, coming from the design of team and show in figure 15, is directly mounted on the breadboard and is a monolithic aluminium block with two M6 holes for board installation and six holes for upper plate block.

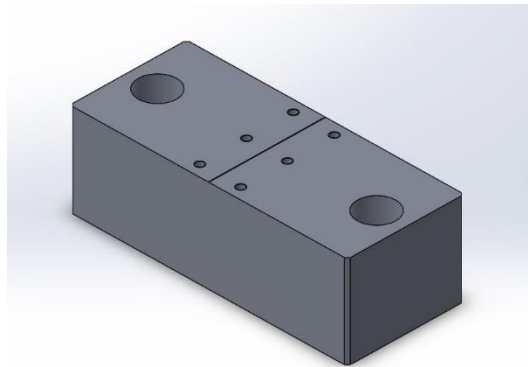Also in this locking system is applied a medium layer of rubber.
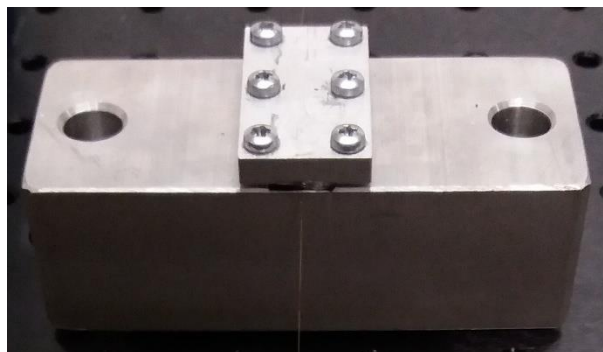

Figure 22: Locking System 2 - Bottom Base

Figure 23: Locking System 2 - Manifactured

It should be noted that on each bottom base, a v-groove of about 1/10 mm in depth has been made to host a part of fiber optic and to permit the correct alignment. Is possible to see the grove as the horizontal center line visible in the figure 17.

It is essential not to do a deeper groove: insert the fiber completely located inside of it not permitting the correct lock of itself.
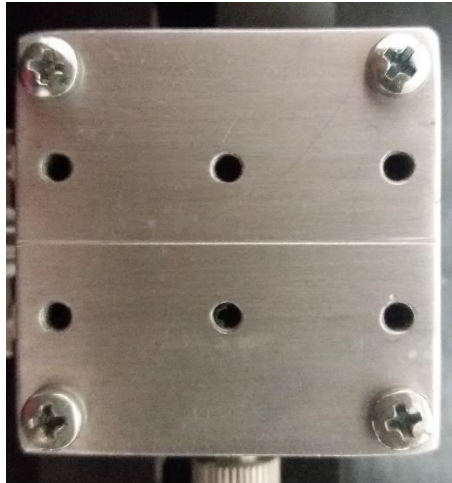

Figure 24: V-Groove

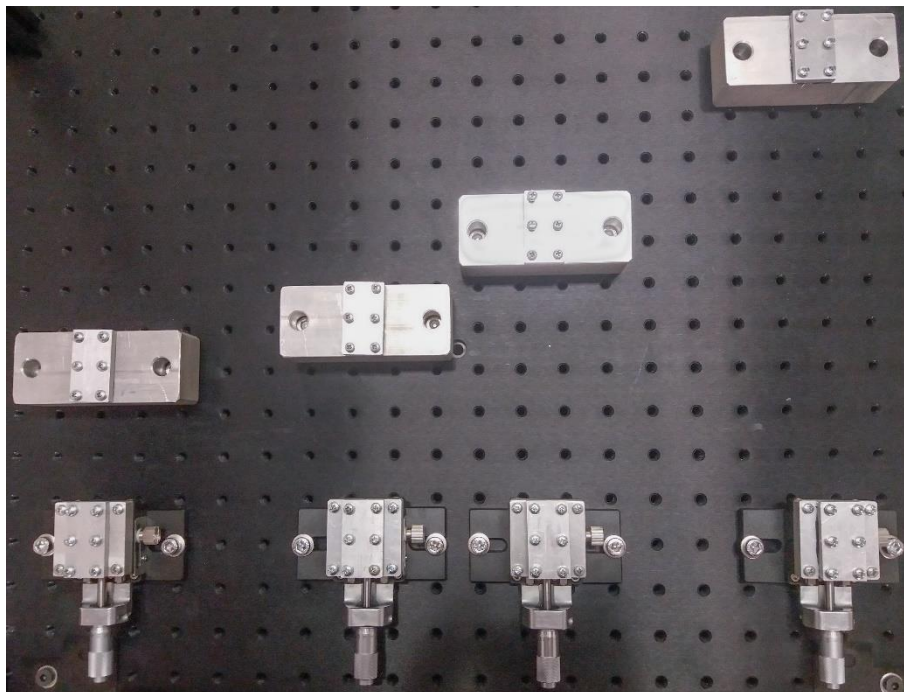The final manufactured set up of the testbench is show in figure 18.

Figure 25: Final Assembly

As already said, different length configurations permit us to study the response of the FBG sensors in strain variations applied by the micro translation stage.

Therefore, the strain values measured change based on the L_0 that is the initial length of the fiber optic on each line.

A general adjustment need to be adopted during the mounting of locking systems: it is necessary avoid hand humidity and dust contamination that can emphasize fiber sliding on the component. So, a properly surface preparation with alcohol and the use of a pair of gloves during fiber handling are strong recommended.

5.2.2 3D-Printed Locking System

In a next phase of the study, it was possible to use a 3D Printer.

This is a big update for the project: according to today's engineering approach, that link the technological grow with a cost containment, the access to additive manufacturing technology allow us to obtain components in a shorter time and a lower cost.

Furthermore, 3D print permit to create complex structure and this give the possible to project complex locking stage in which the lock medium is the epoxy glue like Araldite 2021.

The material used by the 3D Printer is the Polylactid Acid (PLA).

Like the aluminium locking system is composed by two elements: one located on the translation stage and one directly mounted on the breadboard.
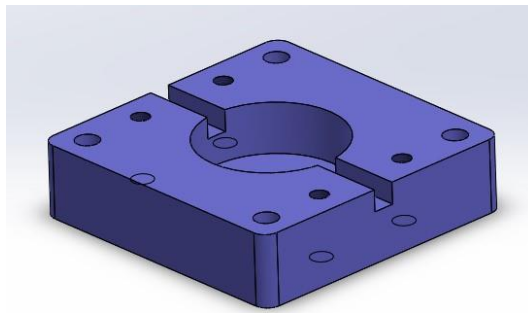

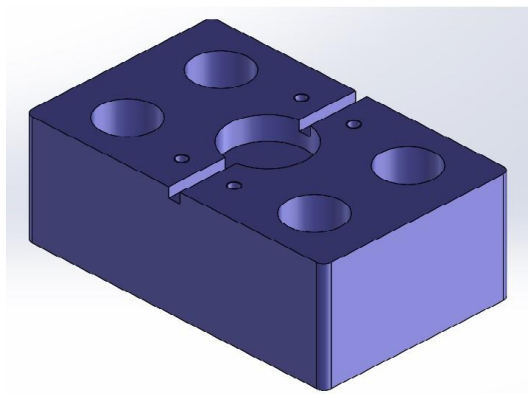*Figure 26: Base on MicroTraslation Stage*

Figure 27: Base on Breadboard

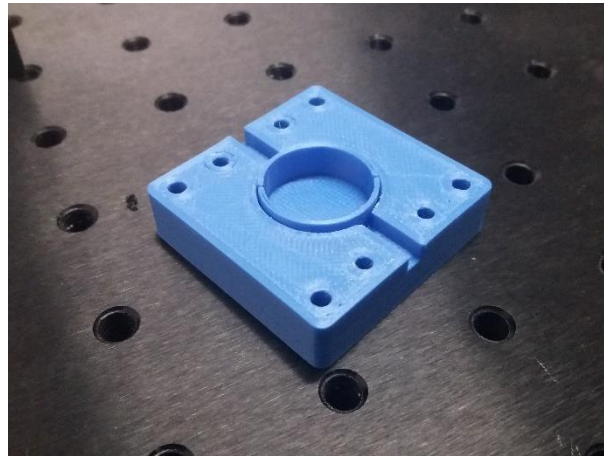Manufactured products are shown in figures 21 and 22:

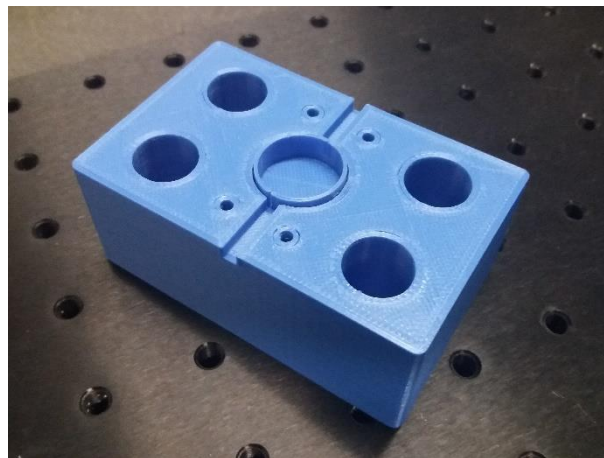*Figure 28: Manifactured 3D Microtraslation Stage*

Figure 29: Manufactured 3D Base on Breadboard

The main feature of new locking systems is a central circular hole where is installed a container where we cast the resin to lock the fiber inside it. Therefore, in the figure 23, are highlighted two cuts created to permit the fiber crossing. The fiber is tensioning along the line and a glue casting fills the "button" totally. A small pressure is applied to avoid the formation of air bubbles in the molecular structure of the resin.

Under big strain loads the container could escape from the hosting hole. So, a plate is locked over it to avoid escape and to reduce the vibration in the hole caused by imperfect match. The 3D printer at our disposal doesn't have a big accuracy.
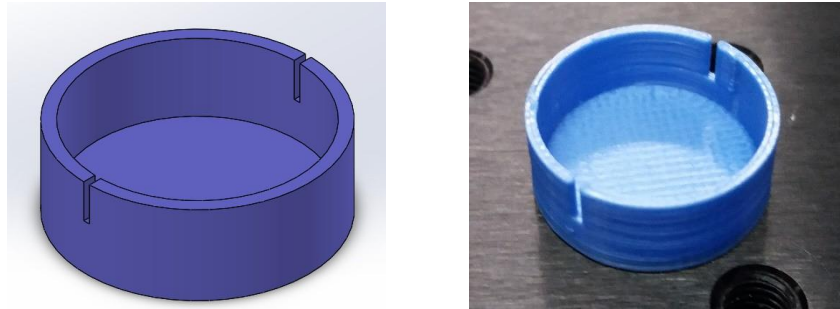

Figure 30: Resin Container

The use of a removable container allows us to substitute easily and quickly the fiber line in case of fiber break during strain test or just if we want to change the fiber under test. The second locking system is composed by two rectangular plats, show in figure 24, where the fiber is leaning and pasted on it.

In this case, if the fiber breaks you should try to remove mechanically resin glued on the plats, but this operation could cause the damage of the component. So, new rectangular plats have to be printed. Also in this case permit the interchangeability of fiber optics, so if you need to use a new fiber, it is necessary to print other rectangular plats.
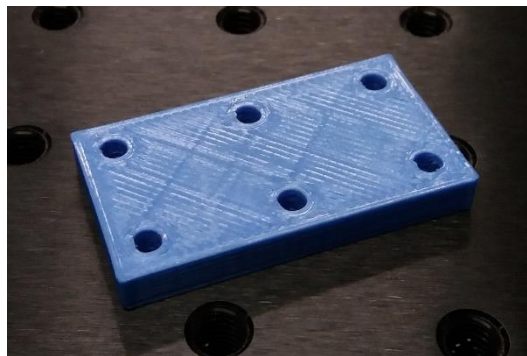
Figure 31: Rectangular Plate

The manufactured set-up is show in figure 25:
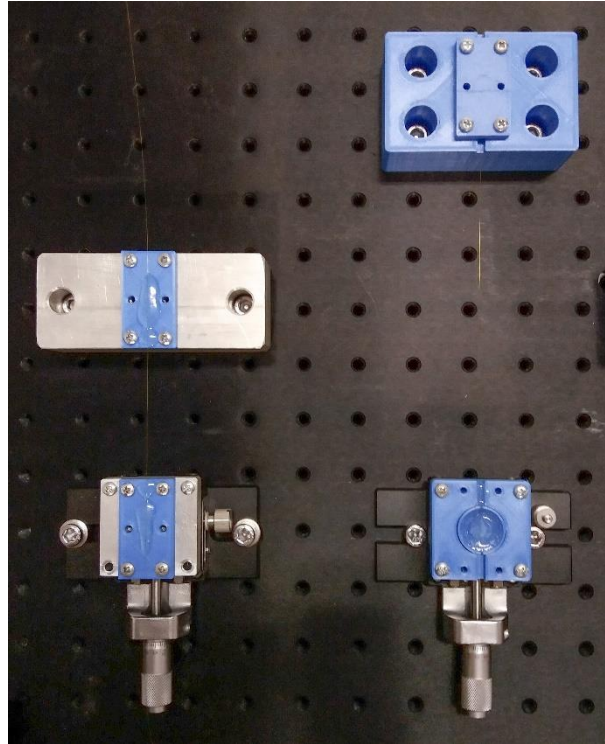
Figure 32: Final Concept

As can be seen, the locking systems are mounted with different value of L_o.
In this way, it is possibile to study how measurements change in response to strain applied by micro translation stage and study how the strain values change in respect of the initial lenght L_o.
Moreover, two lines are mounted with the same L_o but with the two different concept of locking system to permits us to study the quality of those concept fixed L_o.

5.3 Locking System for Thermal Testing

For thermal testing, two different locking systems were designed and manufactured.
Both concepts are a package of three components in which the first is based on a base to host Peltier module, a component to locate fiber optic and a component to insert the temperature sensor.
Like the strain locking, a V-groove of about 1/10 mm in depth is made to accommodate the fiber in the own base.
The depth of groove for Peltier module[10], has not to be much deeper because the cold and hot side of it must keep in touch with the Aluminium component but they have to be separated to not counter the module works. To achieve this condition and to avoid module crashing under locking load some spacers are mounted on the structure.
The package is bolted by using four threaded bars and four nuts, and it is mounted on the breadboard.
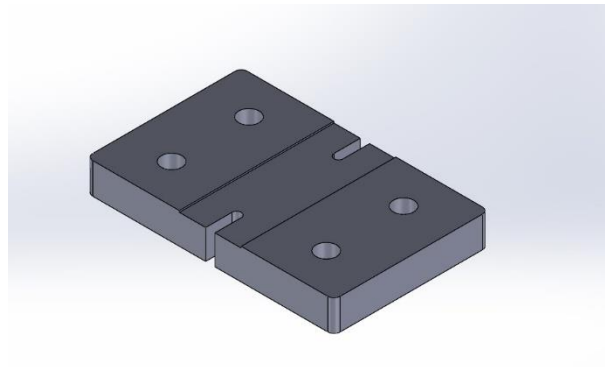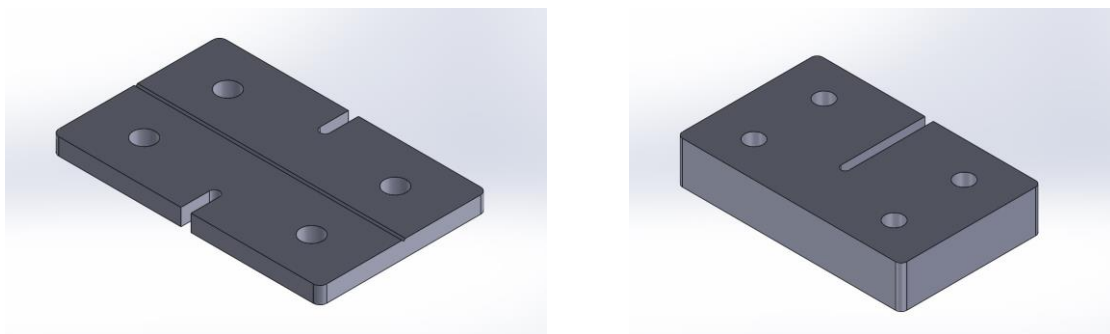

Figure 33: Peltier Module Casing

Figure 34: Fiber And PT100 Temperature Sensor Housing

---

[10] **Peltier Module**: A Peltier heat pump is a solid-state active heat pump which transfers heat from one side of the device to the other, with consumption of electrical energy, depending on the direction of the current.

The second concept is quite similar to the first one. The difference is the design of the base for Peltier module in figure 28. A central threaded hole (*M20*) is to bolt a bar and the Peltier module is located on the end of the threaded bar. This solution permits to approach the thermal module slowly until it touches the upper base where is located the fiber to avoids the module crushing.
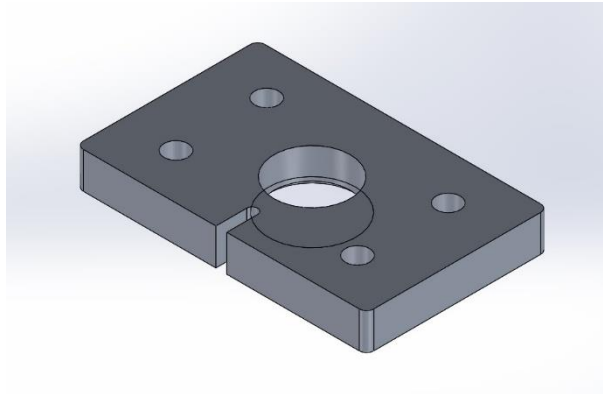
Figure 35: Peltier Casing - Type 2

Aluminium is the chosen material for all elements of the system to avoid different coefficients of thermal expansion that complicates the thermal diffusion model use to analysis the casing.

The use four threaded bars and nuts is a design choice to permit the regulation in height of the entire block. A correct of alignment of the thermal unit with the locking system will be essential in further tests when a thermal-strain combined analysis will be performed.

Figure 36: Final Product Manufactured

5.4 Splicing of Fiber Optics

Splicing is the act to join two optical fibers using heat. The target is to fuse the two fiber together in a way that light passing the fibers is not scattered or reflected by the splice. The splice and the surrounding zone is like an intact fiber.

The heat source is usually an electric arc.

Fusion splicing required expensive equipment but achieve a high accuracy level with low signal quality losses.

Fiber joining is a milestone in the assembly of the test bench. In fact, the fiber with the photoetched FBG doesn't have the interrogator pin connector so it is necessary splice the fiber with a patchcord equipped with the right connector.

To allow the splicing, at first, it is necessary to remove the external coating of the two elements.

The external coating of the patchcord is composed by plastic, acrylate and Kevlar and can be remove using a stripper while for the fiber, having a polyimide coating, two solutions can be used:

1. Heat Source
2. Chemistry Agent such Isoprophyl Alcohol

Once external coating is removed, it is necessary to clean the ends of each fiber and cut off the and with a manual or automatic *cleaver*, show in figure 30. The cleaving process is critical because the ends of each fiber needs to be more perpendicular as possible to the longitudinal fiber axis to avoid optical loss.
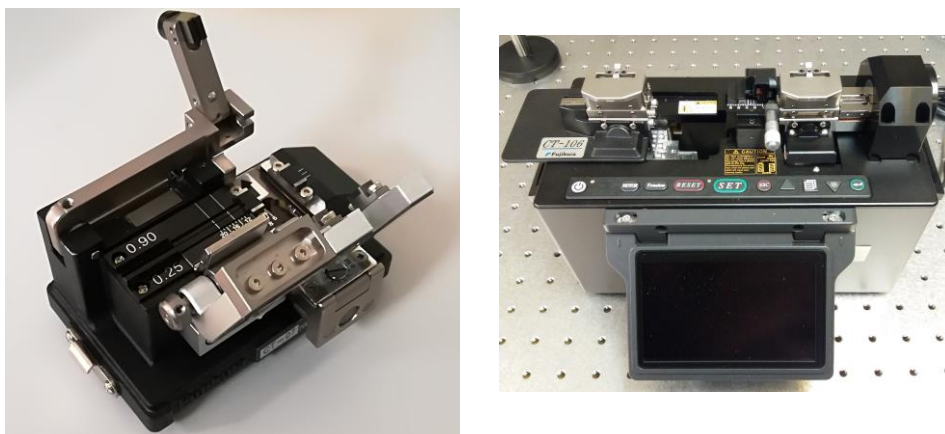
Figure 37: Manual and Automatic Cleaver

After cleaning and cutting, a heat shrinkable tube has to be insert to protect the join that is "naked".

Then, the two fiber optics have to be located inside the *splicer* correctly in proximity to the electrodes, see figure 31.

Figure 38: Fiber Optic Splicing Positioning

During the splicing process you can see the status of fiber optics and the entire process on the machine monitor, see figure 32. After a checking of fiber aligning, the splicing starts.

At the end of this process, an estimated splice loss is displayed on the monitor.

Figure 39: Splicing Process - Visualization and Estimation Loss

5.5 Interrogation System

The "core" of the test bench is the interrogation system.

The interrogator to our disposal is the *SmartFiber SmartScan*.

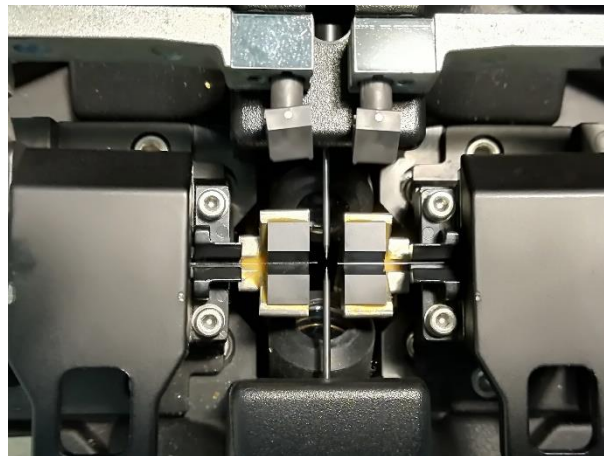SmartScan is an ultra-compact and robust interrogator for dynamic measurement of FBG sensors. This Wavelength Division Multiplexing (WDM) instrument is based on an agile, tuneable laser source that enables high resolution interrogation at multi kHz frequencies. The high frequency scan rates allow oversampling and averaging to give extraordinary resolution.

Figure 40: SmartScan

The main features are show in Table 2.

Measurement and Processing	SmartScan
Wavelength Range	40 nm (1528 – 1568 nm)
Number of Optical Channels[1]	1, 2, 3, 4
Maximum Number of Sensors/Channel	16
Scan Frequency (all sensors simultaneously)	2.5 kHz
Maximum Scan Frequency (with reduced wavelength range)	25 kHz
Repeatability	< 1 pm
Wavelength Stability	< 5 pm over operating temperature range, ± 20 pm over 25 years
Dynamic Range (total tolerable optical attenuation without loss of performance)	27 dB
Dynamic Range (laser launch power minus detection noise floor)	37 dB

Gain Control	9 levels, per channel or per sensor, automatic or user controlled
Onboard Processing	For conversion of measuring units and interfacing to client systems
Bragg Grating Full Width Half Maximum (FWHM)	Minimum > 0.2 nm, > 0.5 nm recommended

Table 2: SmartSoft SmartScan Main Features

The interrogator is supplied with the *SmartSoft* suite, a LabVIEW based application. Smartsoft is a software that allows:

- Advanced Data Logging and Post Acquisition Analysis
- Graphical Representation of Monitoring Systems
- Report Generation and Event Logging
- Integration and Networking of different Instrumentation
- Remote Communication using a variety of Industrial Protocols.
- Automated data reporting to web sites and via email

Even if the acquisition software can show us directly strain and temperature measured, the output of interrogation system is a .log file containing only "raw" (not averaged) Wavelengths.

The .log, as show in next section, will be loaded and post-processed in a *Matlab* software specially for this purpose.

This choice was taken according to Professor Davide Luca Janner of the Department of Applied Science and Technology to get more accurate data as possible due to impossibility of knowing averaging and rounding process of the software.

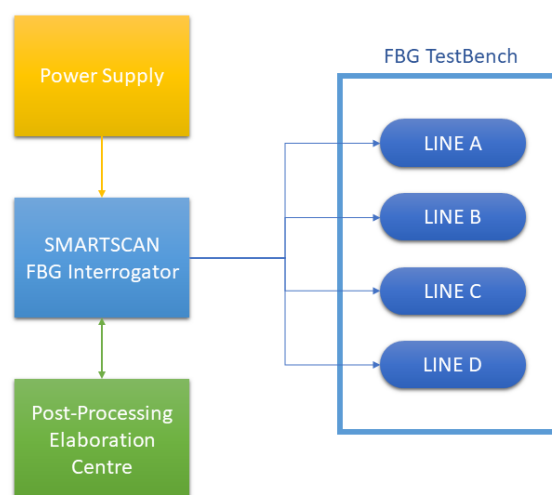The final layout of the testbench if summarized in figure 34.

Figure 41: Final TestBench Layout

6. Self-Developed Software

This chapter is about the Matlab script developed ad-hoc to process row data received by the interrogator.

Even if the instruments are equipped with a software able to give as output a number of useful processed data, we decided to develop our tool to calculate the values we need using raw data to overcome the misalignment the built-in software is affected.

6.1 Software Structure

According the good practices of programming, our self-developed software is made up of the three standard phases:

- *Pre-Processing;*
- *Processing;*
- *Post-Processing.*

Going throw the phases, we can have a better understanding of the process:

Pre-Processing: the user is asked for specify the input file for data and calculation parameter to be used in Post-Processing phase to evaluate mechanical stress and temperature.

Processing: is the core part of our software in which all calculation are carried on. The *.log* file from the interrogator in imported and data are managed to be associated to the sensor they have been measured by.

Post-Processing: the user can customise the output selecting which channels and sensor put in evidence in the plot. If the option "custom analysis" has been selected, it is possible to plot the comparison between mechanical stress and mechanical stress behaviour under temperature changes.

6.2 Physical Principles

One of our drivers during the script's development has been the will that our software could, one day and with several enhancing, used to manage bigger and more complex sensor equipment. Now, the limit is the interrogator's capability to manage only 4 lines with 10 sensor each, meanwhile the script is able to handle N-channel and N-sensor for channel.

Unfortunately, at the moment, we are not able to handle real-time data. This means that this technology can be used to check the status of the structure only after the sensors

have completed their analysis.

To overcome this limit and reach a real-time check of local deformation we should modify the input file structure. This could be possible only by changing the interrogator's source code applying an ad-hoc controller to manage this kind of data acquisition.

This kind of work hasn't been necessary because of the nature of our mission: a statistical sensors' tuning and imported data analysis.

Our work has been carried on focusing on the calculation of strain values form the wavelength values measured by the interrogator. Using equation Kang [19], we could calculate both the mechanical-stress dependant strain and the mechanical/thermal one. The reference equation used was:

$$\varepsilon_m = \frac{\Delta\lambda_B}{(1 - P_e)\lambda_B}$$

Where:

- ε_m is the mechanical stress;
- $K = 1 - P_e$ is the gauge factor (P_e is the photo-elasticity constant). In our application, its value is 0.78;
- $\Delta\lambda_B$ is the value measured for the wavelength change on mechanical stress sensor.

As all the FGB sensors, the measure of data is not a direct one but is obtained *by delta* with reference to a "zero wavelength" typical of each one sensor and dependant from the building process.

This means that the system needs a little tuning to set the "zero values".

Once the system settings are checked, the values of wavelength are red and the physical data can be calculated.

The used interrogator is equipped by the supplier with a set of built-in instruction developed according out technical specification. Obviously, this kind of industrial information can't be published due to a non-disclosure agreement.

6.3 Functions Description

This section has the task to give a schematic description of our script. Reading the code, it is difficult to set a line between the different parts having differ functions. As usually happen in coding, there is a "transitions" phase from a section of the software to another one so in the following we try to explain the main operations contained in the script, the controls inside it and the logic used during design phase.

6.3.1 Check for the Input Files

The first step done by the script is the check of the working directory.

In this phase the software scans the folder looking for all files used in the following phases. If one or more files are missing (o saved with a wrong format differ form the required *".m"*), a pop-up message with the list of this files appears on the screen.

In this way the user can quickly and easily fix the problem.

6.3.2 Check for the File to be analysed

The script asks to the user to specify the file to be analysed and check if it is present in the working directory. It is important that the file name is wrote correctly, including the format and the different between capitol and standard characters.

It is also asked to the user if add a note to the output file.

6.3.3 Analysis definition

Once all preliminary checks have been done, the script carries on the analysis.

It is possible to choose between "standard" or "custom" one. In the first case, no more actions are required to the user and the final plot will be developed. It worth to be high-lined that this kind of analysis is strongly software-dependant form sensors' settings chosen in interrogator management software *SmartSoft*.

If a "custom" analysis is chosen, the user has a wide range of option that can be modified such as parameters measurement and sensors settings. Furthermore, in this section a recap of major data and used sensor list is shown to the user to facilitate his analysis work.

6.3.4 Fiber Optics Characteristic Selection

In this step the software's default fiber characteristic are shown. Obviously, they are the ones has been used in the testbench. But, to be as flexible as possible, the software allows (within certain limits) to modify these parameters to characterize the type of fiber used.

6.3.5 Sensors' settings

This section of our script runs only if the "custom" analysis is chosen.

The software lists all the *"wavelength"* sensors asking the user to define if each one of them is *"strain"* or *"temperature"* type.

The strain sensor is required to be connected to a temperature one in order to manage the influence of temperature if the equipment should be affected by thermal influence. (This option can be bypassed by the user if the thermal influence wants to be neglected.). The way how the temperature influence on strain sensor is manage by means of the aforementioned connection is quite simple: the temperature sensor gives the measure of

deformation due to the heating meanwhile the strain one gives the overall value. Simply subtracting the firs measure to the second one we have the "pure" value for deformation caused by mechanical stress.

Regarding to nominal wavelength of each sensor, the user can choose to write it manually or eventually the Matlab script can do it automatically. The automatic insertion of nominal wavelength it has been implemented to quicken the processing of data and because it was very difficult to find precisely the correct nominal wavelength.

If you want to show the pre-load condition, you have to write manually the nominal wavelength indicated on datasheet.

Regarding to temperature compensation, the Matlab script permits us to associate a single temperature sensor to an entire sensors group or a single sensor.

6.3.6 Check of Correlations

This part of the code analyses the data structure developed until this statement and ask the user to confirm the correlation set between sensors.

As consequence of the possibility given to the user to develop a "custom" analysis neglecting the influence of temperature on strain sensor, the script is able to plot anyway the graph showing the un-correlated behaviour of strain (it means the value without clear evaluation of thermal component).

Before to show this plot, we decided to make the user is aware of his setting with a pop-up and to give him the possibility to confirm his choices or correct the settings adding a thermal sensor to the analysis.

6.3.7 Data Saving

While it is running, the scrip will create inside the working directory a folder to store the output of the analysis. This folder contains the plots and a .txt file summarising all the information acquired during the analysis with possible notes added by the user. The folder's name comes from a standard procedure and has a common pre-fix followed by the input file's name and information on date and hour.

6.4 Process Logic

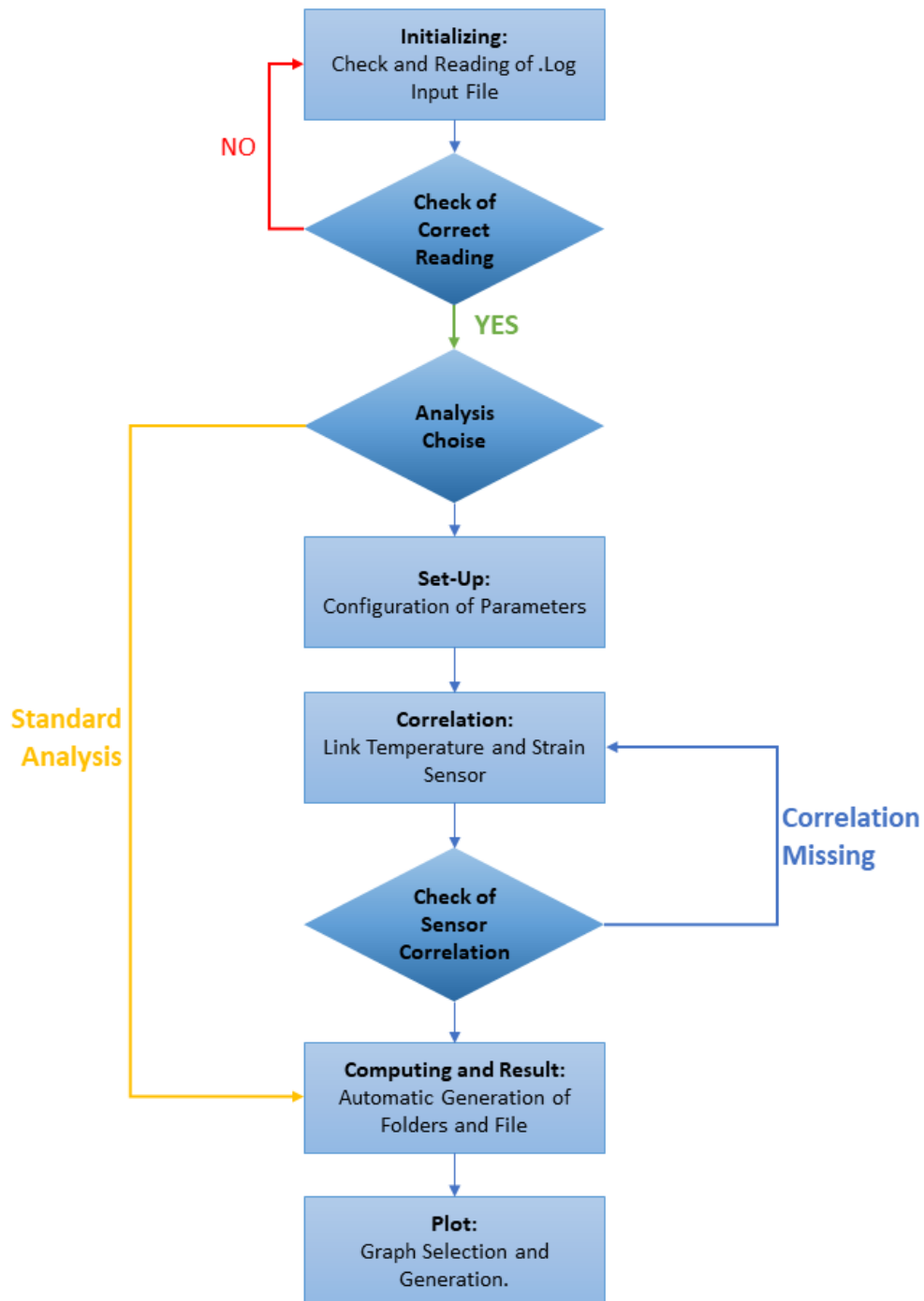To better understand te design logic adopted, a flow chart in shown below in figure 32.

Figure 42: Design Flow Chart

7. Result

By using the acquisition system and the self developed Matlab software for post-processing, it was possible to measure the variations in terms of "raw" wavelength and calculate the strain variations.

All measurements were carried out with a precise logic. In fact, it is a continuous acquisition over time subdivided into ten-seconds blocks in which there are ten seconds of static measurement of wavelenght at the step controlled in terms of ΔL with the micro translation stage and a transient of ten seconds in which the operator moves the micro translation stage to the next controlled step and so on. This alternation of static and transient measurements continue until the end of that given test. The different measurement campaigns allowed us to test both the FBGs and the quality of the locking systems designed.

This chapter presents the most important results obtained for each locking system and by using fiber optic with coating made in Polyimide (preferred to the acrylate one for the better performance).

As explained in the chapter 5, different types of locking systems have been designed and manufactured for the mechanical tests. In particular, these locking systems are mounted on the breadboard by making different lines that varies in length L_o: short, intermediate and a long line have been built.

With regard to the tests performed, statistical analyses were also performed to calculate the corrective coefficient K necessary to correct the measurements affected by errors due to the physical phenomena that will be presented in this chapter. In particular, the step about the evaluation of the corrective coefficient will be shown by presents some significant graphs and tables with the results only for the locking system which contemplates the gluing of the fiber through the use of resin, which give the best result.

7.1 Locking system with Hard Rubber layer

Several cases related to the locking system with the hard rubber layer will be shown and all critical phenomena related to this type of locking system will be explained by showing some important graphs obtained during the measuring campaigns.

7.1.1 Response in terms of strain and wavelength by using the short line L_o=53.59 mm

Incremental load step tests are perfomed by using the locking system equipped with hard rubber layer and mounting the fiber along the short line, characterized by an initial length L_o =53.59 mm.

In this test, the commanded step is of 0.15 mm. It is important to highlight that it is applied a slight preload on fiber optic. The preload is important to make the fiber optic reactive to the commanded step applied by using a microtranslation stage.

The result in terms of strain variations measured and wavelength detected, is shown in the following figure 43. The legend of this graph indicates a standard name in which Ch1 indicates the channel of interrogator and Gr1 indicates the Bragg grating interrogated by on this line. Obviously, the standard name varies based on the channel and grating used.
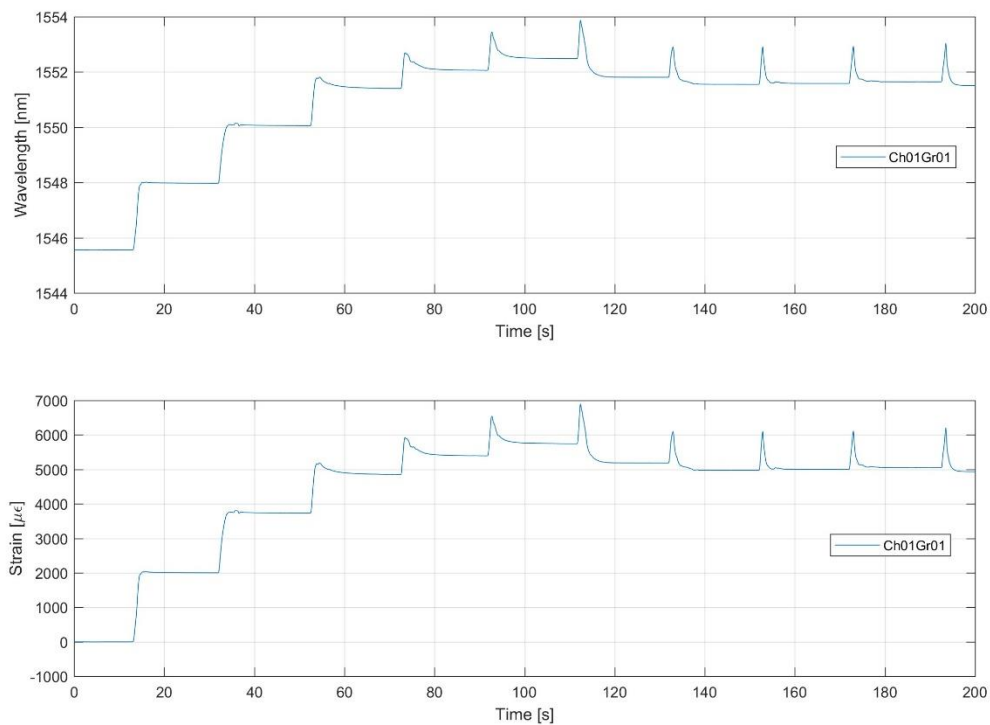

Figure 43: Response in terms of Strain and Wavelength in the Short Line

In this test it is possible to notice that between 0 and about 50 seconds, the controlled steps are well detected. The constant lines represent the controlled steps while the lines with an almost vertical slope are the transients towards the next step.

The graph shows also the main negative phenomena related to this kind of locking system: the sliding of the optical fiber on rubber and aluminium.

In fact, by increasing the load steps, strain measured it should be higher than the measured one. It is noted that from 60 seconds to about 110 seconds the optical fiber slips consistently and from about 110 seconds, and the relative load step, the FBG sensor is completely unusable.

In addition to the sliding of the optical fiber, there are also two other negative phenomena to be considered, namely the deformation of the rubber layer and the creation of a kind of "channel" on the rubber itself. This channel is formed due to the "nature" of the locking system, that is designed to crush the rubber layer on the fiber. The rubber has its softness which creates a tunnel in the structure that causes a further sliding of the fiber.

All these negative phenomena *make inaccurate the measurements obtained*.

As previously written, a statistical analysis was performed for the evaluation of the corrective coefficient of our measurements and it is possible to obtain a graph that shows the data fitting and the theoretical curve. Especially in this case the sliding of the fiber can be seen because the experimental curve does not pass through the origin of the axes but intersect the Y axis.

This, as we will see in the following paragraphs, does not happen in the case of locking system with epoxy resin.

7.1.2 Response in terms of strain and wavelength using the intermediate line L_o=128.80 mm

Regarding to the intermediate line, the response in terms of strain improves.

For this test, the same commanded step of the preview test is applied.

From the graphs shown in figure 44, it is possible to notice how the sliding phenomena is attenuated. This behaviour, compared to the short line before illustrated, is due to that the load per unit length, ad consequentially the strain, is smaller with the same commanded step.

From the graph shown in figure 1.2 it seems that the fiber follows exactly the commanded steps.

Instead, by plotting the two curves experimental and theoretical, in terms of ΔL, we notice the deviation between these two curves immediately, see figure 45.
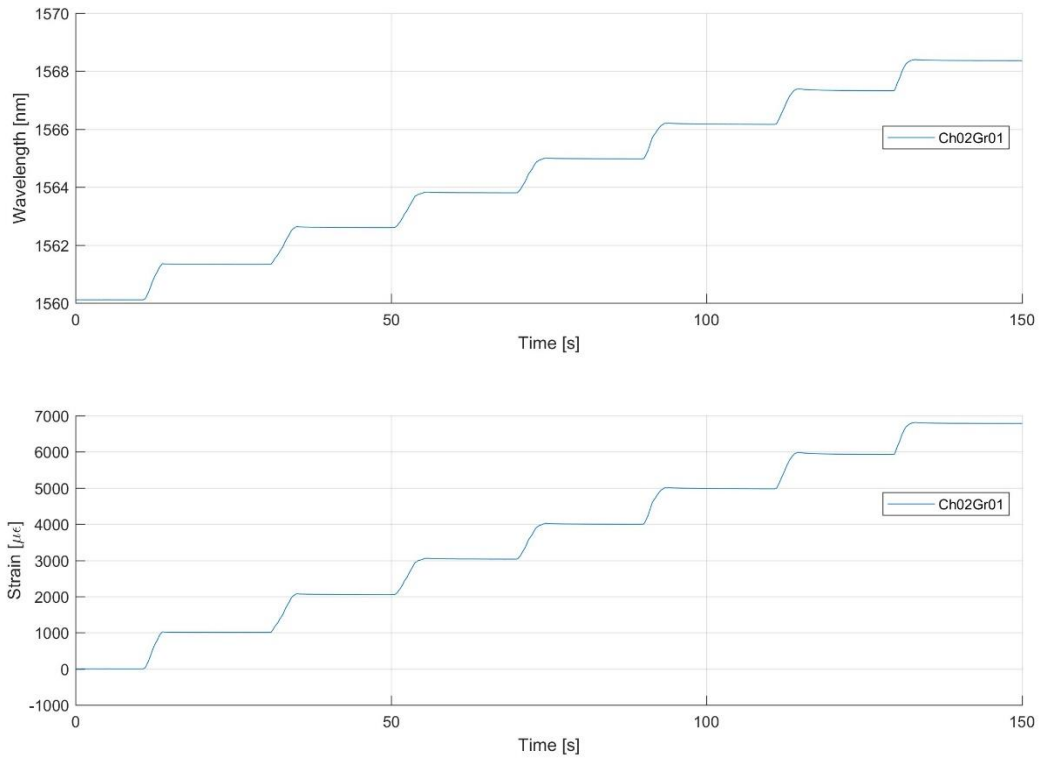

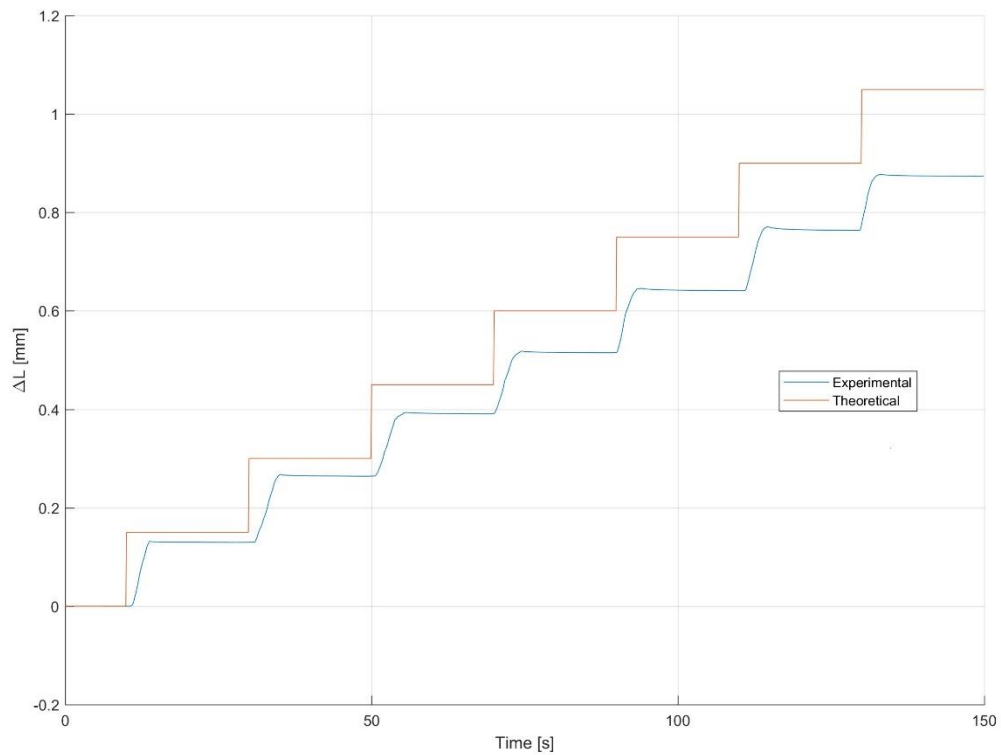*Figure 44: Response in terms of Strain and Wavelength in the Intermediate Line*

Figure 45: Comparison between Theoretical and Experimental Curve - Intermediate Line

The gap in terms of *ΔL* that exists over the test is probably due to the rubber deformation and fiber sliding. However, the sliding with respect to what occurred using the short line, is more attenuated.

7.1.3 Response in terms of strain and wavelength using the intermediate line L_o=228.94 mm

The long line with an initial length of about L_o=228.94 mm and its trend like that for the intermediate line. Obviously, strain is smaller compared to other lines, because the initial length is larger and the step commanded are the same.

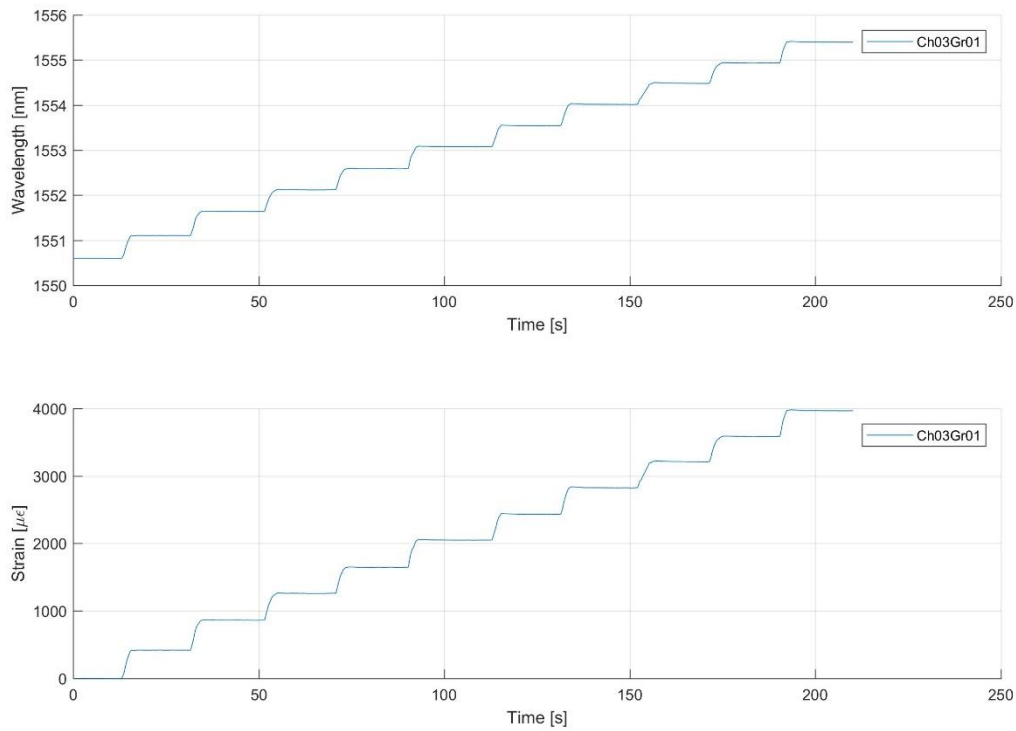This test is performed by commanding a step of 0.10 mm.

Figure 46: Response in terms of Strain and Wavelength in the Long Line

Similarly to the previous case, the graph that shows the deviation between the theoretical and experimental curve.
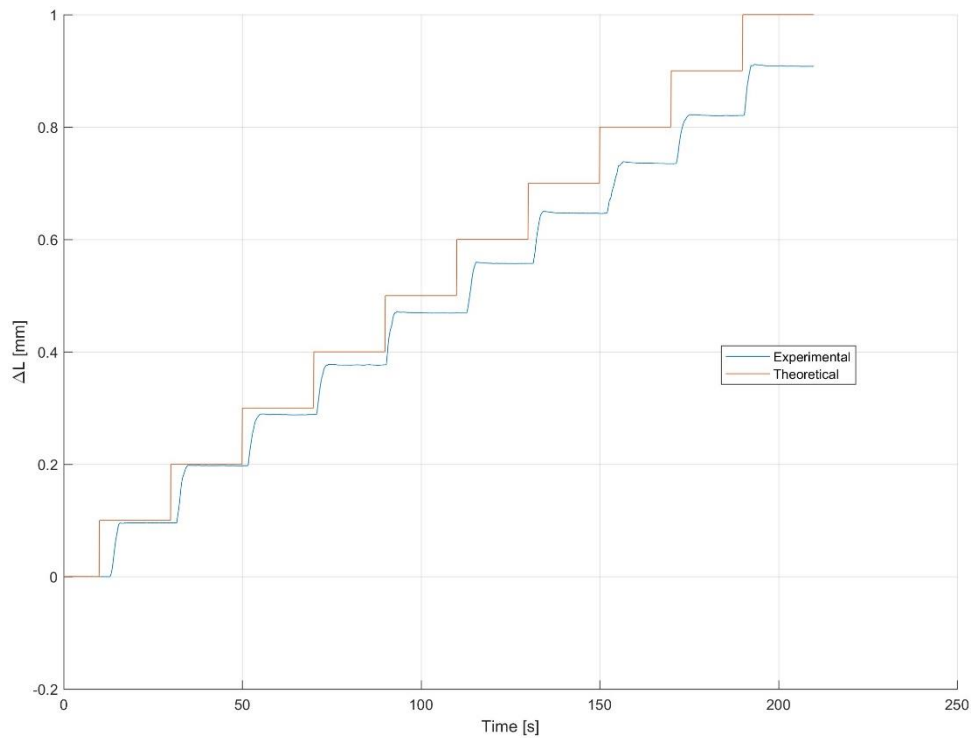

Figure 47: Comparison between Theoretical and Experimental curves - Long Line

As previously written, the response obtained is like the response of the intermediate line, even if for the first steps controlled the system responds well and follows the theoretical trend.

However, by considering the whole test it is possible to notice how the gap in terms of ΔL continues to grow.

7.1.4 Repeatability test with Locking System with Hard Rubber

For locking systems with hard rubber, in addition to performing incremental step tests, repeatability tests were performed by using the long line, because it is the one that shows the best results in incremental step tests. In this test, the commanded step is 0.10 mm.

It is possible to notice how the measure is repeatable but there are gaps not acceptable in terms of ΔL and that make this locking system not reliable.

Therefore, in this test it is clear how the sliding of fiber optic influences the measurements. In fact, when we return to the 0 mm command, rather than returning to this value of command, the detected ΔL is minor of zero.

To understand this phenomenon is important to highlight that the fiber has been preloaded and since it has slipped on the rubber layer, the preload is lost and a wavelength detected is less than the wavelength taken as reference (λ_o).

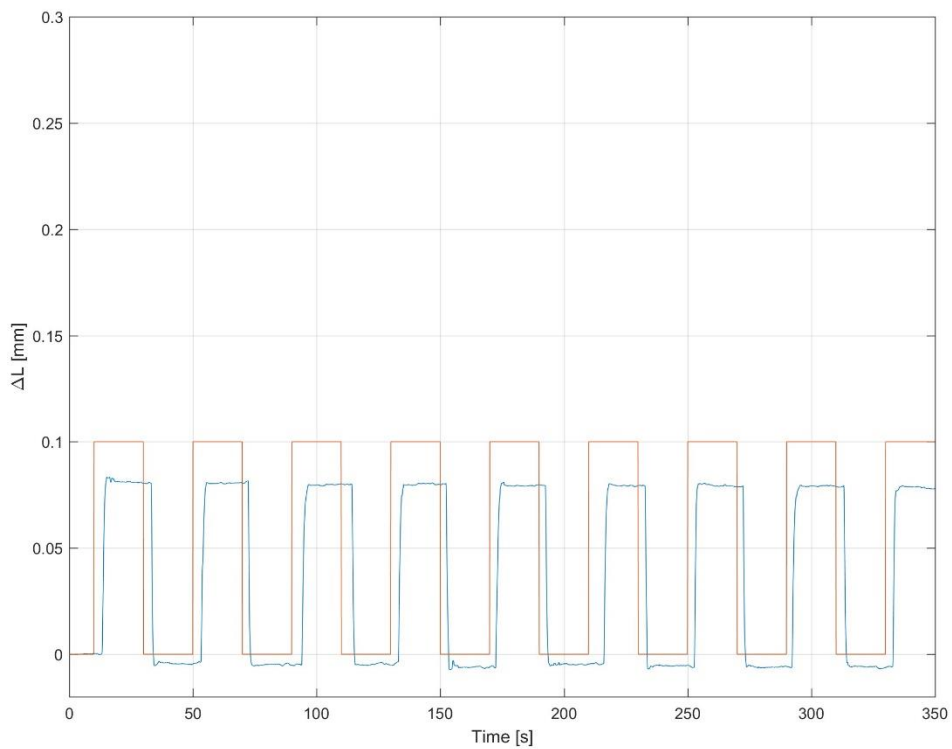The result obtained is shown in the following figure 48:

Figure 48: Repeatability Test with Locking System - Hard Rubber and Long Line

7.2 Locking system with Soft rubber layer

Tests like those performed for the locking system with hard rubber were also performed to test locking systems using soft rubber layer.

As done in the previous section, only the most significant results will be shown.

In particular, only the results obtained with the short and the long line are shown.

7.2.1 Response in terms of strain and wavelength by using the short line L_o=53.59 mm and the long line L_o=228.94 mm

The first test done is the Incremental load step test and in this test the commanded step is 0.10 mm.

The response in terms of wavelength and strain is presented in the following figure 1.7. From the graph obtained it is possible to notice how the fiber is subject to a continuous sliding on the soft rubber.
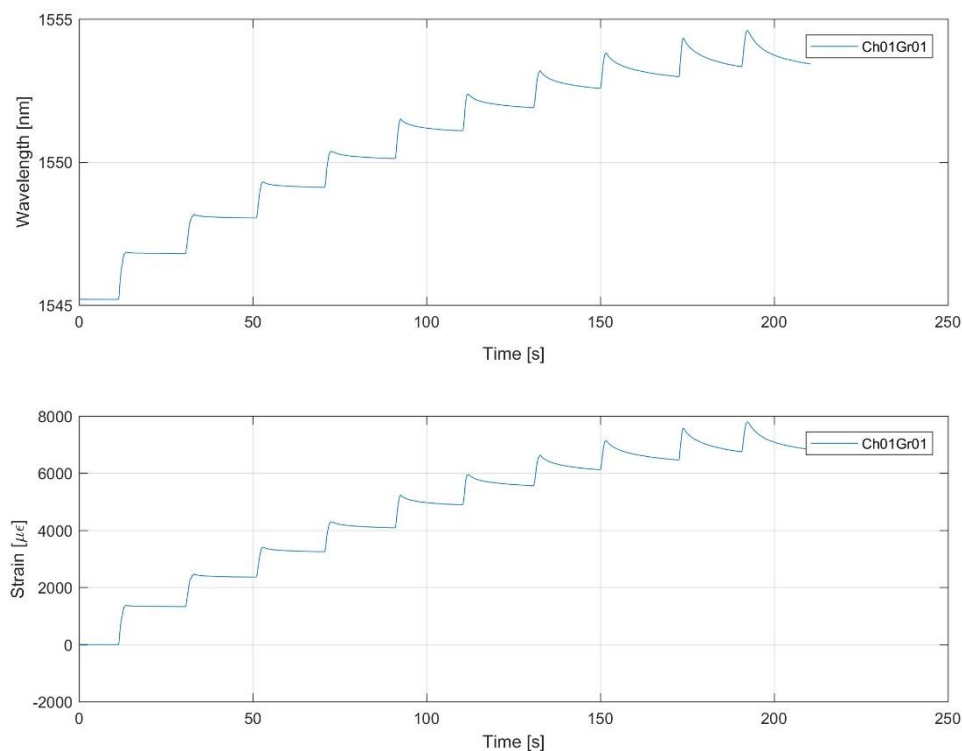

Figure 49: Incremental Test with Locking System with Soft Rubber - Short Line

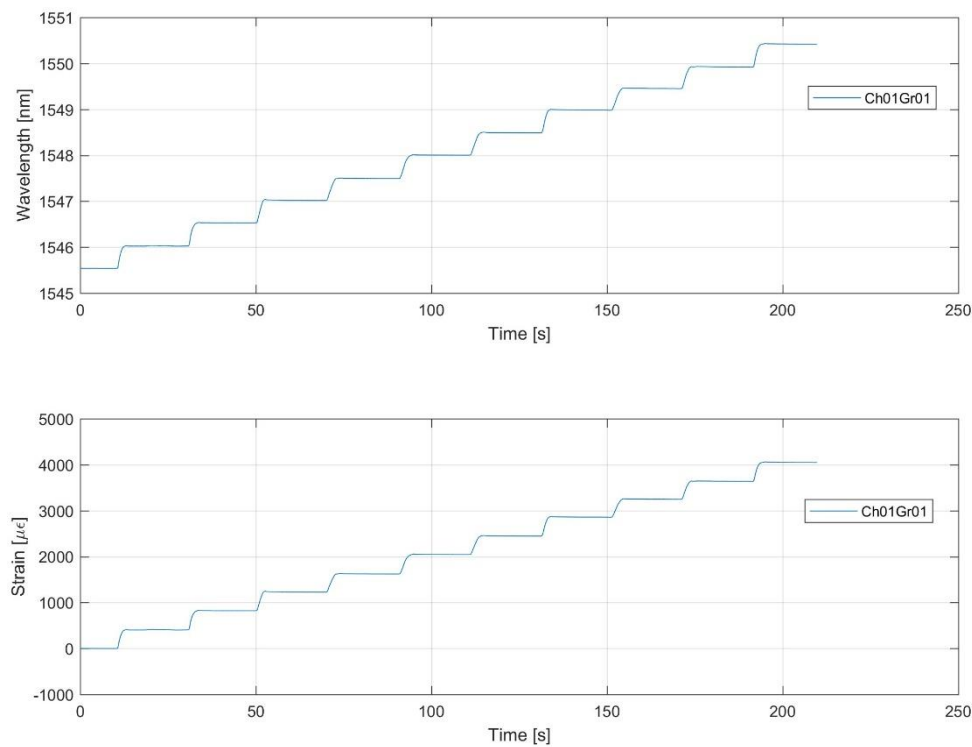Regarding to the long line, it has been obtained the following figure 50:

Figure 50: Incremental Test with Locking System with Soft Rubber - Long Line

The fiber optic, mounted on the long line, response correctly to the commanded step. Unfortunately, this behaviour is repeatable but the sliding of the fiber optic on rubber layer is clear.

To study this behaviour, a repeatability test was performed and also in this test a slight preload is applied:
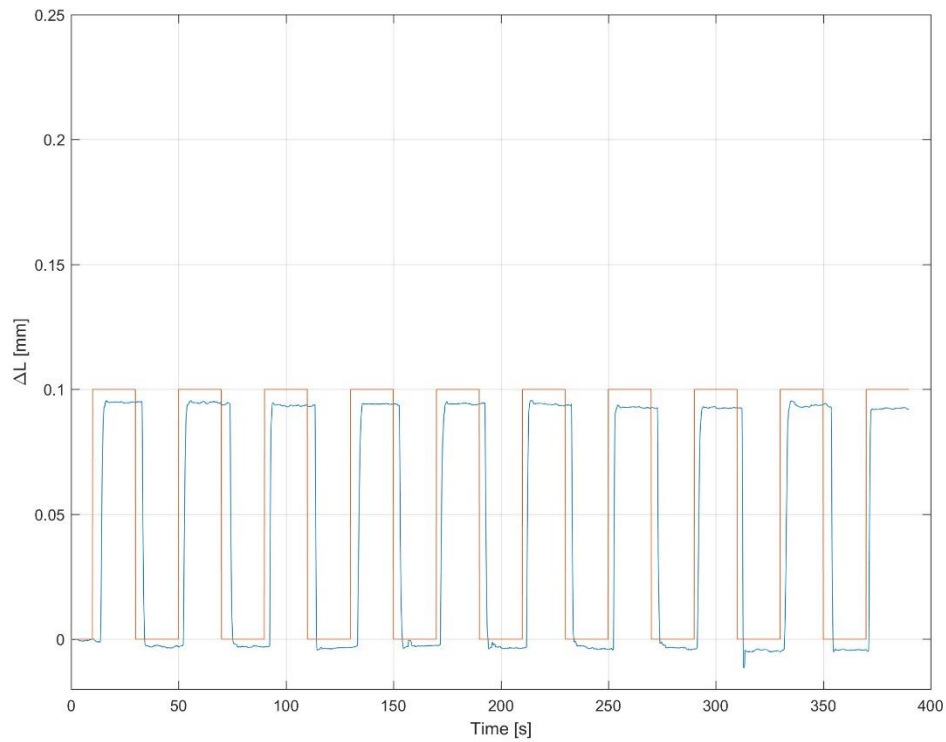

Figure 51: Repeatability Test with Locking System - Soft Rubber and Long Line

7.3 Locking System with Epoxy Glue

Several mechanical tests have been done by using the locking systems manufactured by 3D printing. Therefore, these tests have been conducted to study the quality of two different concepts of locking systems explained in chapter 5.

Four different lines are settled on the breadboard: two lines with initial length L_o of about 53.59 mm and 228.94 mm by gluing fiber on rectangular plats and two parallels lines with initial length L_o of about 151.16 mm one of which the fiber is glued on rectangular plats while the other is attached by using the locking systems with the container.

It is important to highlight that all tests are performed by *pre-loading* the fiber optic to have a responsive FBG sensor.

7.3.1 Comparison between Two Concepts of Locking Systems

This measuring campaigns starts with the study of response in terms of strain variations by varying locking system.

Consequently, the two parallel lines with the same length and different locking systems are used.

First, a repeatability test was performed with 0.10 mm as commanded step.

The results obtained about this repeatability test are shown in figure 1.10. The *Ch01Gr01* is relative to the first channel with the fiber mounted using the locking system with containers and the *Ch02Gr01* is relative to the other line with locking system based on rectangular plats.

In Figure 53 it is possible to notice how the 0 mm steps are very well detected by sensor, and not for the 0.1 mm steps. Probably is due to the deformation of the glue used to lock the fibers and the deformation of the coating.

However, these negative phenomena are reversible and it is possible to understand it: removing the load the sensor detects 0 mm.

This aspect did not happen with the locking systems with rubber layers. Hence, if the experimental curve (blue line) cannot to reach the command of 0.1 mm, it is mainly due to elastic phenomena of epoxy resin. In fact, the resin can deform itself because of the fiber optic stretching.

At the end, it should be noted that sometimes the experimental blue curve does not return to 0 mm because there are negative effects caused by parallax errors and in the command given by operator.
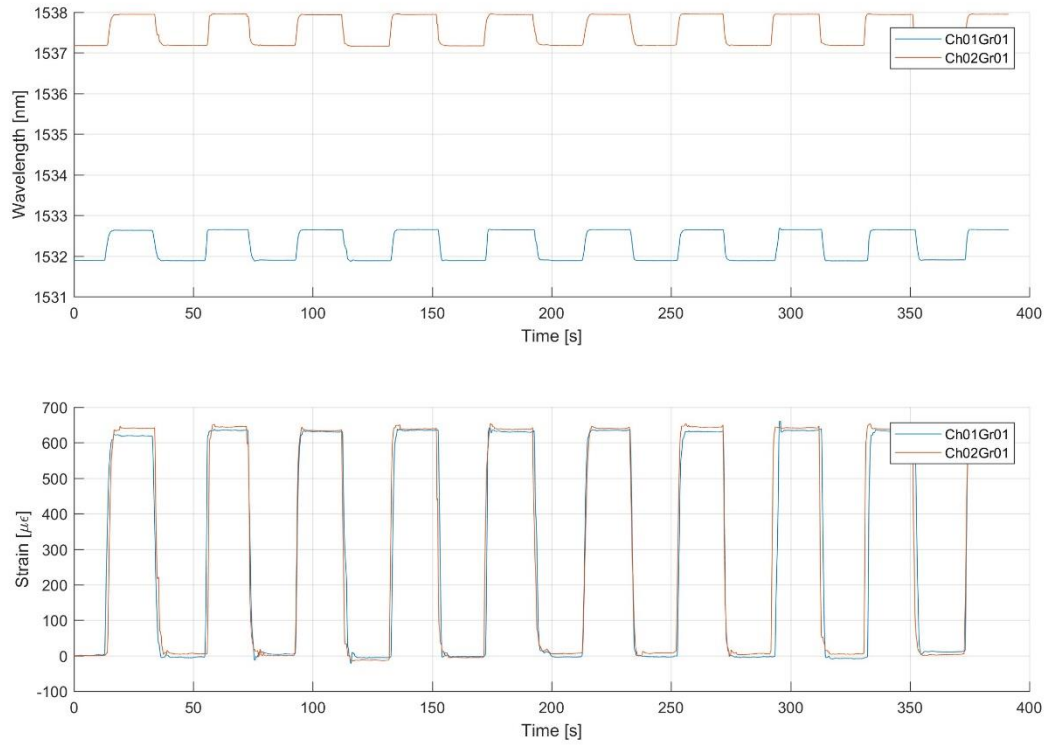
Figure 52: Repeatability Test - Locking System Hard Rubber

For these tests to compare the quality and for a numerical evaluation of the phenomena explained above, corrective coefficients ($K_{corrective}$) are computed.

Unfortunately, a small number of tests have been performed but they are sufficient to give a preliminary evaluation of K_{mean} and the error $ΔK$ associated. As performed for locking system with a rubber layer, the corrective coefficient has been computed with incremental load step tests by commanding a step of 0.05 mm.

Some graphs are shown to see the experimental and theoretical curves and how the corrective coefficient acts on the experimental results obtained, see figures 1.11 and 1.12.
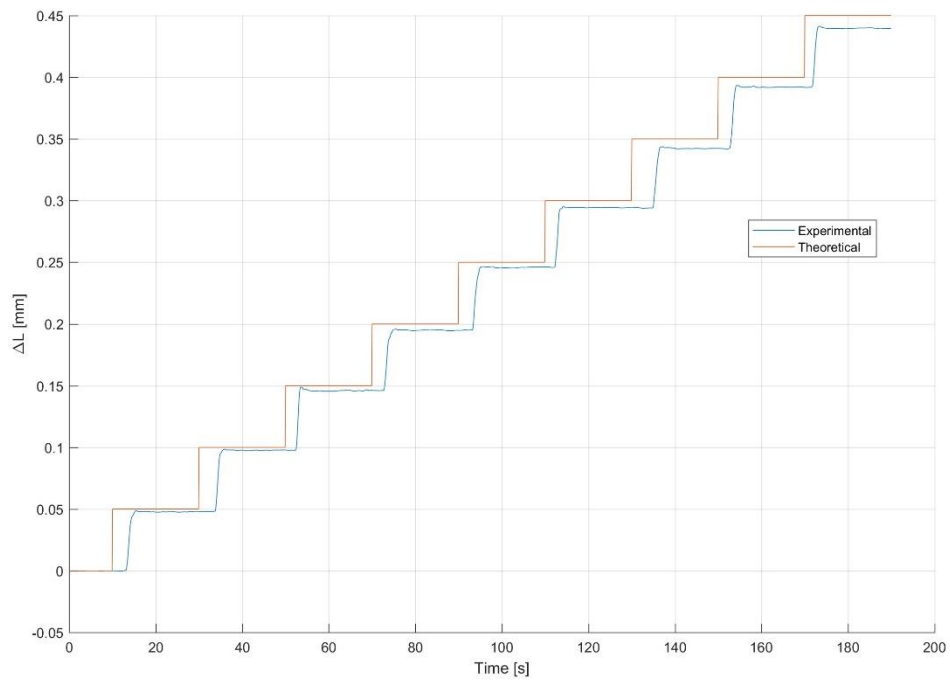
Figure 54:: Comparison between Theoretical and Experimental Curves – No Corrective Coefficient
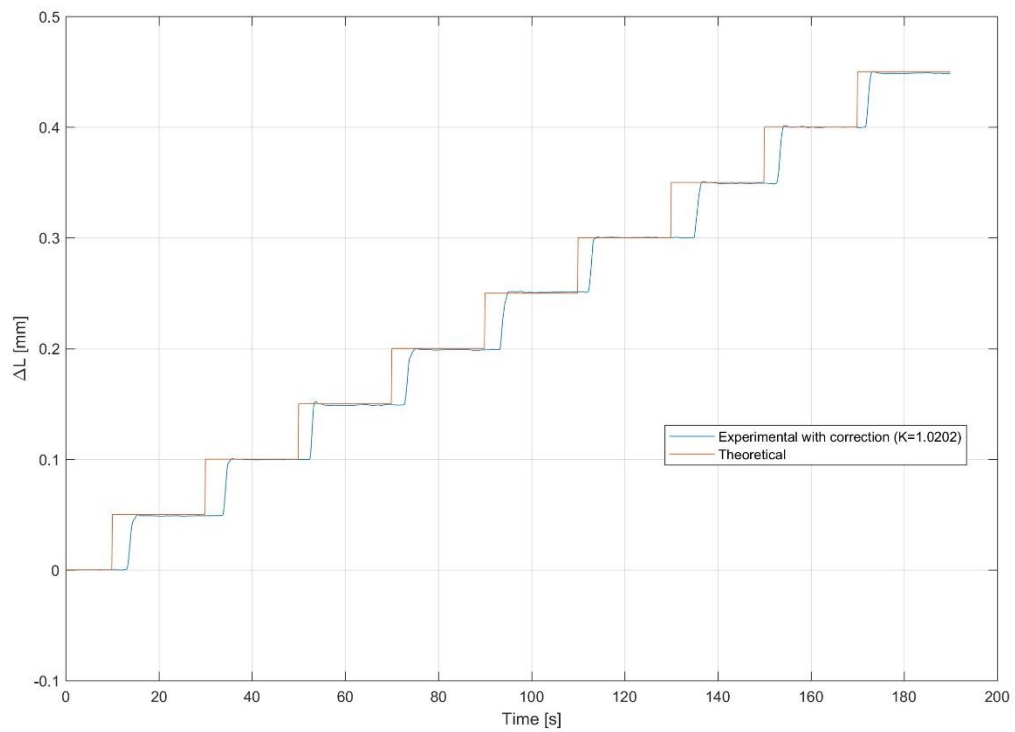

Figure 53: Comparison between Theoretical and Experimental Curves - Corrective Coefficient

As explained previously, the measurements were made following a precise logic, in which ten seconds of measurement of wavelength to a fix steps commanded are alternated with ten seconds of transient in which the operator takes to the next step. For this reason, the graphs show a step pattern.

Regarding to plot the linear fit, per each ten seconds of measurement of wavelength, fixed the step commanded, mean values of wavelength are computed and these values minus the average wavelength Y-coordinate (Δλ) values were used to obtain the experimental curves created by using the linear fit. Each ten second blocks contain 100 values of detected wavelengths and each value is subtracted from the nominal wavelength. Then, obtained these values, average values of wavelength are computed and these values represent the Y coordinates of the points, instead the X coordinates are the commands in terms of strain variations commanded with the micro translation stage.
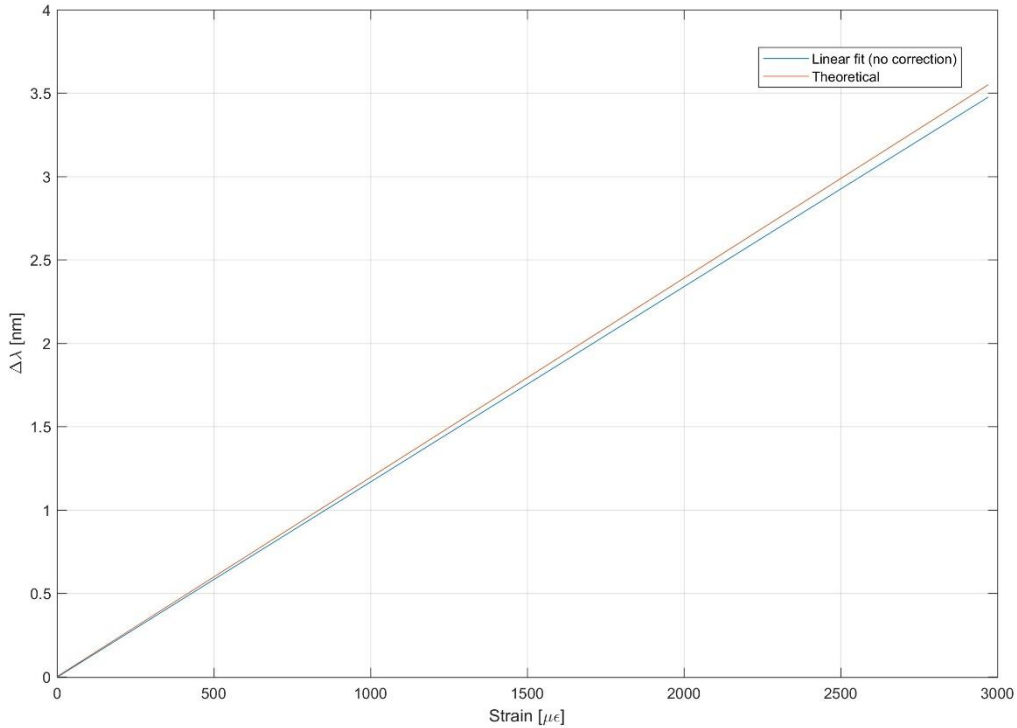

Figure 55: Comparison between Theoretical and Experimental Trend - No Corrective Coefficient

To be able to make a comparison between the theoretical curve and the curve of the data fitting, all the ten seconds blocks related to the transients have been discarded, because they are not important in our analysis.
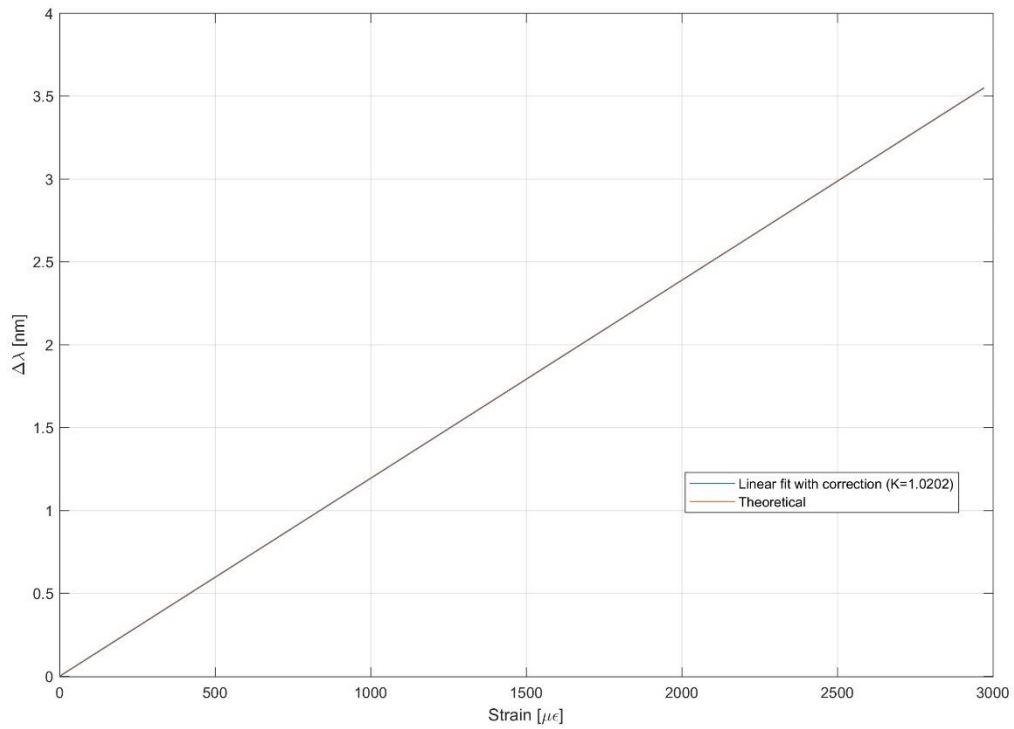
Figure 56: Comparison between Theoretical and Experimental Trend - Corrective Coefficient

In the following tables are shown all results get:

Corrective Coefficient Values	
$K_{corrective}$	$K_{mean} \pm \Delta K$
1.0263	
1.0202	1.0212 ± 0.0045
1.0173	
1.0209	

Table 3: Corrective Coefficient Values - Plate Locking System

Corrective Coefficient Values	
K_corrective	$K_{mean} \pm \Delta K$
1.0377	
1.0359	
1.0357	1.0350± 0.0011
1.0337	

Table 4: Corrective Coefficient Values - "Container" Locking System

In K_{mean} are included all phenomena about deformation of fiber coating and epoxy resin. Instead, the ΔK is relative to the command and to parallax error.

7.3.2 Conclusion

A little difference in value between two K_{mean} can be underlined.

The second type of locking system (codenamed "container") is characterized by a higher value of K_{mean}. Probably, it is caused by a higher quantity of epoxy resin used to lock the fiber optics and by a non-completed fiber surrounding by epoxy resin (so, a part of the fiber can be directly in touch with the plat).

To achieve best result and confirm our hypothesis, it is recommended to do other tests to have a solid data sets.

It is possible to conclude that, in terms of strain variation, the systems are equivalent and guarantee almost the same response.

7.3.1 1.3.3 Comparison between two different line: L_o=53.59 mm and L_o=228.94 mm

To estimate how L_o can influence measurements, some tests have been done by using two different fibers glued on two different lines.

It is important to highlight that the values of L_o are not standardized and it is due to the mounting of locking systems on the breadboard. Four tests increasing the load steps of 0.05 mm have been done to obtain four corrective coefficients showed in the following tables.

Corrective Coefficient Values	
$K_{corrective}$	$K_{mean} \pm \Delta K$
1.1403	
1.1140	1.1248 ± 0.0132
1.1180	
1.1270	

Table 5: Corrective Coefficient Values - Short Line

Corrective Coefficient Values	
$K_{corrective}$	$K_{mean} \pm \Delta K$
1.0021	
1.0026	1.0012 ± 0.0013
1.0002	
1.0000	

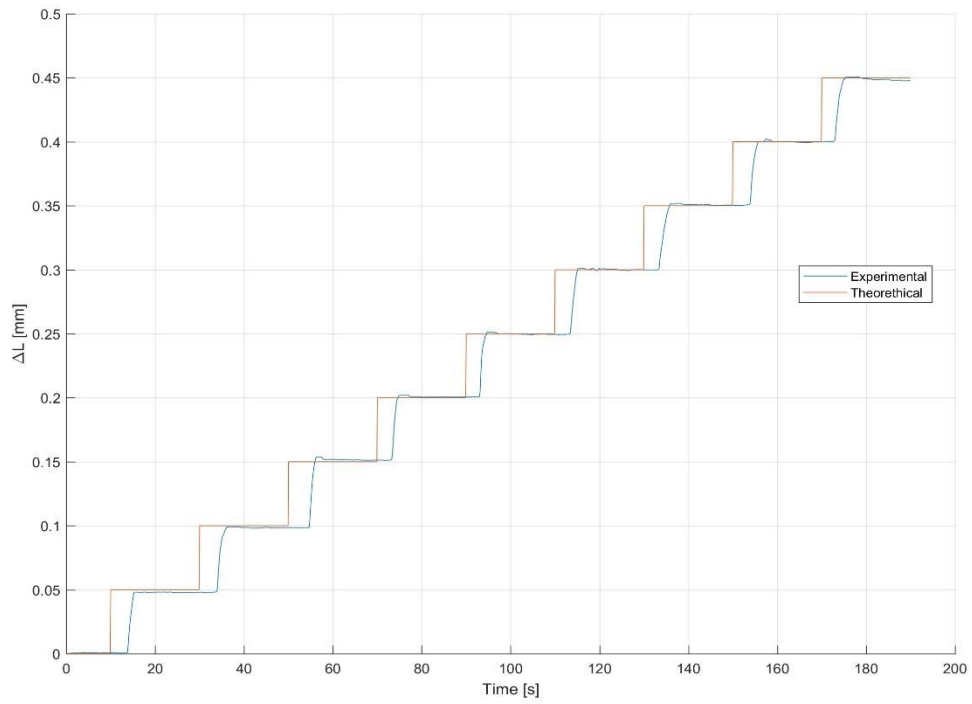*Table 6: Corrective Coefficient Values - Long Line*

Figure 57: Comparison between Theoretical and Experimental Trend - Increasing Load Steps
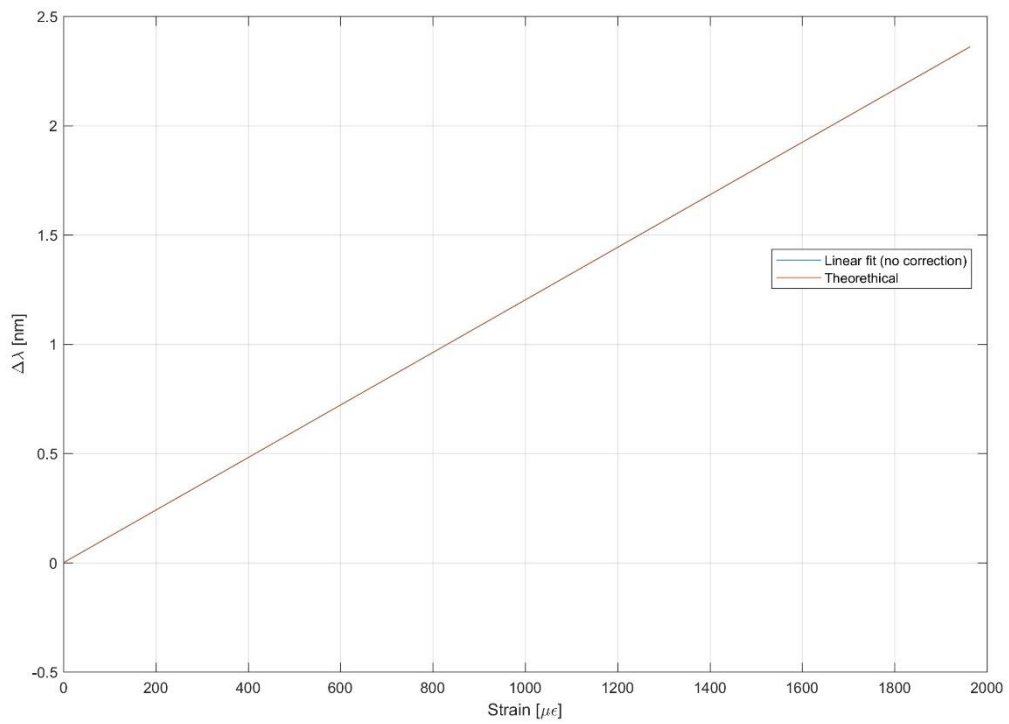

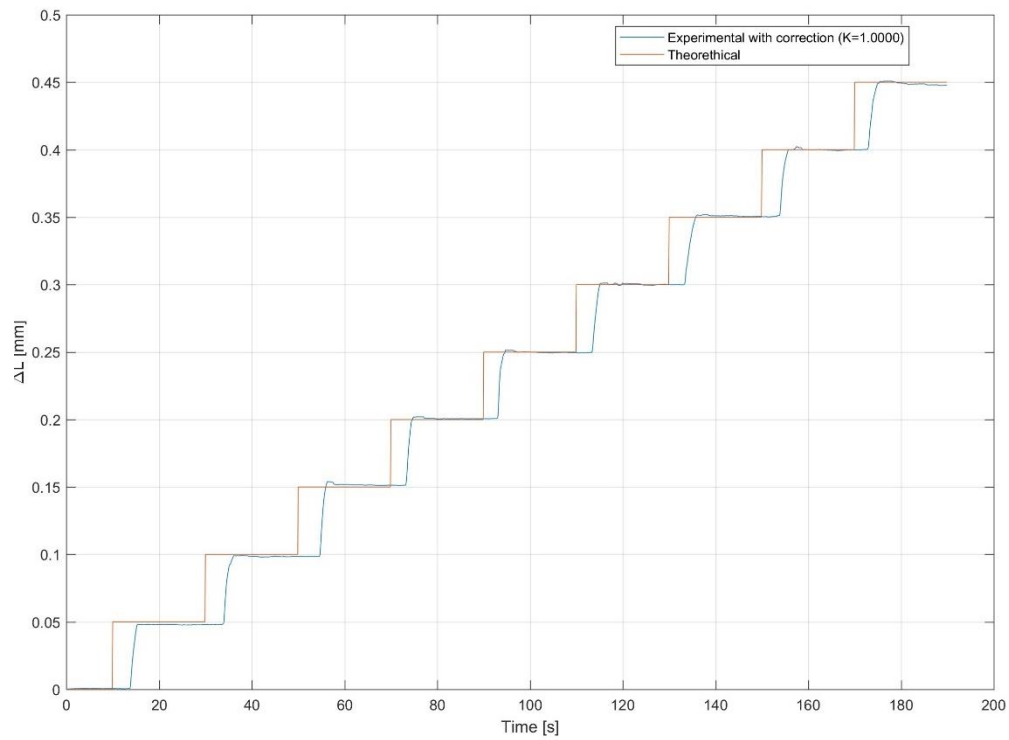*Figure 58: Comparison between Theoretical and Experimental Trend – Linear Fit*

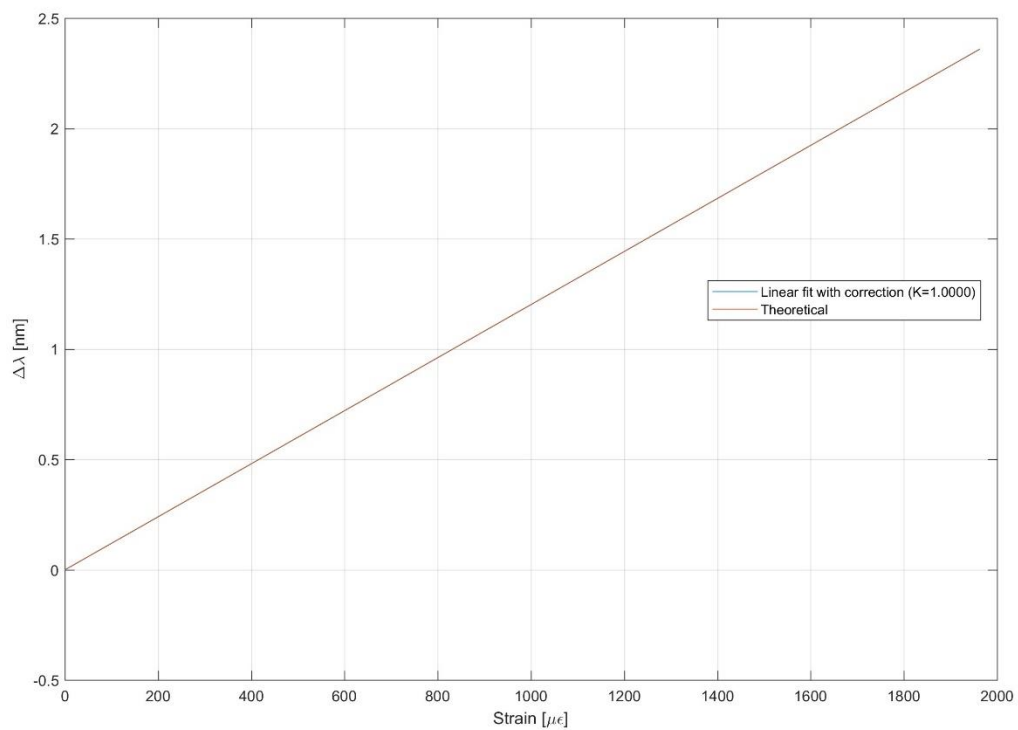*Figure 59: Comparison between Theoretical and Experimental Trend – Corrective Coefficient*

Figure 60: Comparison between Theoretical and Experimental Trend – Linear Fit and Corrective Coefficeint

7.3.1   Conclusion about the comparison between two different L_o

According to the tests performed, it is noted that the fiber mounted on a short line presents a critical behavior. This is due to the fact that with the same command but with a small initial length L_o, the strain is larger.

For this reason, gluing becomes more deformed. The best solution turns out to be the system with L_o = 228.94 mm and in general with L_o large because they guarantee a good response. Obviously, by having the same command and having a larger L_o, the resin is subject to smaller strain.

7.3.2 Repeatability Test with long line L_o=228.94 mm by varying the pre-load

Focusing the long line, three repeatability tests are performed. In particular these tests differ from value of preload that are, in terms of ΔL, 0.30 mm, 0.20 and 0.10 mm.

It is possible to notice that by reducing the amount of preload, the response in terms of strain variations is better and the experimental curve accurately follow the theoretical curve.

8. Acknowledgements

I would first like to thank my thesis main supervisor Professor Paolo Maggiore of the Department of Mechanical and Aerospace Engineering. Together with my co-supervisor Matteo Dalla Vedova, they were always a continuous support during the research activity with patience, motivation and immense knowledge. Their guidance helped me in all time of thesis and it was essential to overcome the difficult moments.

My sincere thanks also go to Prof. Daniel Milanese and Prof. Davide Janner, who, according with my advisor, provided me the opportunity to join the *Photonext* team, and who gave access to the *Istituto Superiore Mario Boella*.

Besides of them, I should like to say special thanks to dott.ssa Nadia Boetti that support us in the fiber splicing with an immense serenity and joy. Without her support it would not be possible to conduct this research.

I thank also my lab mates, Giancarlo and Andrea, for the hard work and the application during our research. It was nice working with you guys!

Last but not the least, I would like to thank my parents and my brother for the constant and unconditional support throughout every day of my life. Their guidance and encouragements has always been aimed to allowing me to express myself in the best possible conditions. They were enormously inspirational for me and I hope they are proud of me, now and in the future.

9. Bibliography

[1]   R. Kashyap, *Fiber bragg gratings*. Academic press, 2009.

[2]   S. Kumar and M. J. Deen, *Fiber optic communications: fundamentals and applications*. John Wiley & Sons, 2014.

[3]   H. Murata, "Handbook of optical fibers and cables," 1996.

[4]   G. P. Agrawal, *Fiber-optic communication systems*, vol. 222. John Wiley & Sons, 2012.

[5]   M. Yamane and Y. Asahara, *Glasses for photonics*. Cambridge University Press, 2000.

[6]   Wikipedia contributors, "Numerical Aperture," *Wikipedia, The Free Encyclopedia.* [Online].
Available:
https://en.wikipedia.org/w/index.php?title=Numerical_aperture&oldid=8420766
59. [Accessed: 20-Jul-2018].

[7]   Wikipedia contributors, "Modal Dispersion," *Wikipedia, The Free Encyclopedia.* [Online].
Available:
https://en.wikipedia.org/w/index.php?title=Modal_dispersion&oldid=791733186
. [Accessed: 22-Jul-2018].

[8]   B. E. A. Saleh, M. C. Teich, and B. E. Saleh, *Fundamentals of photonics*, vol. 22. Wiley New York, 1991.

[9]   S. O. Kasap and R. K. Sinha, *Optoelectronics and photonics: principles and practices*, vol. 340. Prentice Hall New Jersey, 2001.

[10]   Wikipedia contributors, "Diffraction Grating." .

[11]   F. Colpo, L. Humbert, and J. Botsis, "An experimental numerical study of the response of a long fibre Bragg grating sensor near a crack tip," *Smart Mater. Struct.*, vol. 16, no. 4, p. 1423, 2007.

[12]   E. Tessadori, "Misure di deformazione e temperatura mediante sensori a fibra ottica: tecniche di disaccoppiamento del segnale," 2012.

[13]   C. Chojetzki, M. W. Rothhardt, J. Ommer, S. Unger, K. Schuster, and H.-R. Mueller, "High-reflectivity draw-tower fiber Bragg gratings—arrays and single gratings of type II," *Opt. Eng.*, vol. 44, no. 6, p. 60503, 2005.

[14]   R. S. Figliola and D. E. Beasley, "Theory and design for mechanical measurements." IOP Publishing, 2001.

[15]   I. S. O. Vim, *International vocabulary of basic and general terms in metrology (VIM)*, vol. 2004. 2004.

[16]   J. S. Bendat and A. G. Piersol, *Random data: analysis and measurement procedures*, vol. 729. John Wiley & Sons, 2011.

[17]   K. Bury, *Statistical distributions in engineering*. Cambridge University Press, 1999.

[18]   Wikipedia contributors, "Sorbothane," *Wikipedia, The Free Encyclopedia.* [Online].
Available:
https://en.wikipedia.org/w/index.php?title=Sorbothane&oldid=788998004.
[Accessed: 19-Jun-2018].

[19]   M.-K. Kang, D.-J. Park, and S.-S. Lee, "Strain measurements on a cantilever beam

with fiber bragg grating sensors using a pair of collimators," *Int. J. Precis. Eng. Manuf.*, vol. 13, no. 3, pp. 455–458, 2012.

[20]   Wikipedia contributors, "Magnitude," *Wikipedia, The Free Encyclopedia.* [Online]. Available: https://en.wikipedia.org/w/index.php?title=Magnitude_(mathematics)&oldid=830873479. [Accessed: 23-Apr-2018].

[21]   Wikipedia contributors, "Fiber Bragg Grating," *Wikipedia, The Free Encyclopedia.* [Online]. Available: https://en.wikipedia.org/w/index.php?title=Fiber_Bragg_grating&oldid=830844973. [Accessed: 23-Apr-2018].